

Unbiased Hamiltonian Monte Carlo with couplings

Jeremy Heng* and Pierre E. Jacob*

August 28, 2018

Abstract

We propose a methodology to parallelize Hamiltonian Monte Carlo estimators. Our approach constructs a pair of Hamiltonian Monte Carlo chains that are coupled in such a way that they meet exactly after some random number of iterations. These chains can then be combined so that resulting estimators are unbiased. This allows us to produce independent replicates in parallel and average them to obtain estimators that are consistent in the limit of the number of replicates, instead of the usual limit of the number of Markov chain iterations. We investigate the scalability of our coupling in high dimensions on a toy example. The choice of algorithmic parameters and the efficiency of our proposed methodology are then illustrated on a logistic regression with 300 covariates, and a log-Gaussian Cox point processes model with low to fine grained discretizations.

Keywords: Coupling, Hamiltonian Monte Carlo, Parallel computing, Unbiased estimation.

1 Introduction

1.1 Parallel computation with Hamiltonian Monte Carlo

Hamiltonian Monte Carlo is a Markov chain Monte Carlo method to approximate integrals with respect to a target probability distribution π on \mathbb{R}^d . Originally proposed by [Duane et al. \[1987\]](#) in the physics literature, it was later introduced in statistics by [Neal \[1993\]](#) and is now widely adopted as a standard sampling tool [[Brooks et al., 2011](#), [Lelièvre et al., 2010](#)]. Various aspects of its theoretical properties have been studied: see [Betancourt et al. \[2017\]](#) and [Betancourt \[2017\]](#) for its geometric properties, [Livingstone et al. \[2016\]](#) and [Durmus et al. \[2017\]](#) for ergodicity results, [Beskos et al. \[2013\]](#), [Mangoubi and Smith \[2017\]](#) and [Bou-Rabee et al. \[2018\]](#) for scaling results with respect to the dimension d . These results suggest that Hamiltonian Monte Carlo compares favorably to other Markov chain Monte Carlo algorithms such as random walk Metropolis–Hastings and Metropolis-adjusted Langevin algorithms in high dimensions. In practice, Hamiltonian Monte Carlo is at the core of the No-U-Turn sampler [[Hoffman and Gelman, 2014](#)] which is implemented in the software Stan [[Carpenter et al., 2016](#)].

If one could initialize from the target distribution, usual estimators based on any Markov chain Monte Carlo would be unbiased, and one could simply average over independent chains [[Rosenthal, 2000](#)]. Except certain applications where this can be achieved with perfect simulation methods [[Casella et al., 2001](#), [Huber, 2016](#)], Markov chain Monte Carlo estimators are ultimately consistent in the limit of the number of iterations. Algorithms that rely on such asymptotics face the risk of becoming obsolete if computational power continue to increase through the number of available processors and not through clock speed.

*Department of Statistics, Harvard University, USA. Emails: jjmheng@fas.harvard.edu & pjacob@fas.harvard.edu.

Several methods have been proposed to address this limitation with varying generality [Mykland et al., 1995, Neal, 2002, Glynn and Rhee, 2014]. Our approach builds upon recent work by Jacob et al. [2017], which introduces unbiased estimators based on Metropolis–Hastings algorithms and Gibbs samplers. The present article describes how to design unbiased estimators for Hamiltonian Monte Carlo and some of its variants [Girolami and Calderhead, 2011]. The proposed methodology is widely applicable and involves a simple coupling between a pair of Hamiltonian Monte Carlo chains. Coupled chains are run for a random but almost surely finite number of iterations, and combined in such a way that resulting estimators are unbiased. One can produce independent copies of these estimators in parallel and average them to obtain consistent approximations in the limit of the number of replicates. This also yields confidence intervals valid in the number of replicates through the central limit theorem; see also Glynn and Heidelberger [1991] for central limit theorems parametrized by number of processors or time budget.

We begin by introducing some preliminary notation in Section 1.2 and recapitulating the unbiased estimation framework of Jacob et al. [2017] in Section 1.3.

1.2 Notation

Given a sequence $(x_n)_{n \geq 0}$ and integers $k < m$, we use the convention that $\sum_{n=m}^k x_n = 0$. The set of natural numbers is denoted by \mathbb{N} and the set of non-negative real numbers by \mathbb{R}_+ . The d -dimensional vector of zeros is denoted by 0_d and the $d \times d$ identity matrix by I_d . The Euclidean norm of a vector $x \in \mathbb{R}^d$ is written as $|x| = (\sum_{i=1}^d x_i^2)^{1/2}$. Given a subset $A \subseteq \Omega$, the indicator function $\mathbb{I}_A : \Omega \rightarrow \{0, 1\}$ is defined as $\mathbb{I}_A(x) = 1$ if $x \in A$, and 0 if $x \in \Omega \setminus A$. For a smooth function $f : \mathbb{R}^d \rightarrow \mathbb{R}$, we denote its gradient by $\nabla f : \mathbb{R}^d \rightarrow \mathbb{R}^d$ and its Hessian by $\nabla^2 f : \mathbb{R}^d \rightarrow \mathbb{R}^{d \times d}$. The gradient of a function $(x, y) \mapsto f(x, y)$ with respect to the variables x and y are denoted by $\nabla_x f$ and $\nabla_y f$ respectively. Given functions $f : \mathbb{R}^n \rightarrow \mathbb{R}^m$ and $g : \mathbb{R}^d \rightarrow \mathbb{R}^n$, we define the composition $f \circ g : \mathbb{R}^d \rightarrow \mathbb{R}^m$ as $(f \circ g)(x) = f\{g(x)\}$ for all $x \in \mathbb{R}^d$. The Borel σ -algebra of \mathbb{R}^d is denoted by $\mathcal{B}(\mathbb{R}^d)$; on the product space $\mathbb{R}^d \times \mathbb{R}^d$, $\mathcal{B}(\mathbb{R}^d) \times \mathcal{B}(\mathbb{R}^d)$ denotes the product σ -algebra. The Gaussian distribution on \mathbb{R}^d with mean vector μ and covariance matrix Σ is denoted by $\mathcal{N}(\mu, \Sigma)$, and its density by $x \mapsto \mathcal{N}(x; \mu, \Sigma)$. The uniform distribution on $[0, 1]$ is denoted as $\mathcal{U}[0, 1]$. We use the shorthand $X \sim \eta$ to refer to a random variable with distribution η . On a measurable space (Ω, \mathcal{F}) , given a measurable function $\varphi : \Omega \rightarrow \mathbb{R}$, a probability measure η , and a Markov transition kernel M , we define the integral $\eta(\varphi) = \int_{\Omega} \varphi(x) \eta(dx)$ and the function $M(\varphi)(x) = \int_{\Omega} \varphi(y) M(x, dy)$ for $x \in \Omega$.

1.3 Unbiased estimation with couplings

Suppose $h : \mathbb{R}^d \rightarrow \mathbb{R}$ is a measurable function of interest and consider the task of approximating the integral $\pi(h) = \int h(x) \pi(dx) < \infty$. Following Glynn and Rhee [2014] and Jacob et al. [2017], we will construct a pair of coupled Markov chains $X = (X_n)_{n \geq 0}$ and $Y = (Y_n)_{n \geq 0}$ with the same marginal law, associated with an initial distribution π_0 and a π -invariant Markov transition kernel K defined on $\{\mathbb{R}^d, \mathcal{B}(\mathbb{R}^d)\}$. To do so, we introduce a Markov transition kernel \bar{K} on $\{\mathbb{R}^d \times \mathbb{R}^d, \mathcal{B}(\mathbb{R}^d) \times \mathcal{B}(\mathbb{R}^d)\}$ that admits K as its marginals, i.e. $\bar{K}\{(x, y), A \times \mathbb{R}^d\} = K(x, A)$ and $\bar{K}\{(x, y), \mathbb{R}^d \times A\} = K(y, A)$ for all $x, y \in \mathbb{R}^d$ and $A \in \mathcal{B}(\mathbb{R}^d)$. After initializing $(X_0, Y_0) \sim \bar{\pi}_0$ with a coupling that has π_0 as its marginals, we then simulate $X_1 \sim K(X_0, \cdot)$ and $(X_{n+1}, Y_n) \sim \bar{K}\{(X_n, Y_{n-1}), \cdot\}$ for all integer $n \geq 1$. We will write pr to denote the law of the coupled chain $(X_n, Y_n)_{n \geq 0}$, and E to denote expectation with respect to pr . We now consider the following assumptions.

Assumption 1 (Convergence of marginal chain). *As $n \rightarrow \infty$, we have $E\{h(X_n)\} \rightarrow \pi(h)$. Furthermore, there exist $\kappa_1 > 0$ and $C_1 < \infty$ such that $E\{h(X_n)^{2+\kappa_1}\} < C_1$ for all integer $n \geq 0$.*

Assumption 2 (Tail of meeting time). *The meeting time $\tau = \inf\{n \geq 1 : X_n = Y_{n-1}\}$ satisfies a geometric tail condition of the form $\text{pr}(\tau > n) \leq C_2 \kappa_2^n$ for some constants $C_2 \in \mathbb{R}_+$, $\kappa_2 \in (0, 1)$ and all integer $n \geq 0$.*

Assumption 3 (Faithfulness). *The coupled chains are faithful [Rosenthal, 1997], i.e. $X_n = Y_{n-1}$ for all integer $n \geq \tau$.*

Under these assumptions, the random variable defined as

$$H_k(X, Y) = h(X_k) + \sum_{n=k+1}^{\tau-1} \{h(X_n) - h(Y_{n-1})\} \quad (1)$$

for any integer $k \geq 0$, is an unbiased estimator of $\pi(h)$ with finite variance [Jacob et al., 2017, Proposition 3.1]. Computation of (1) can be performed with $\tau - 1$ applications of \bar{K} and $\max(1, k + 1 - \tau)$ applications of K ; thus the compute cost has a finite expectation under Assumption 2. The first term, $h(X_k)$, is in general biased since the chain $(X_n)_{n \geq 0}$ might not have reached stationarity by iteration k . The second term acts as a bias correction and is equal to zero when $k \geq \tau - 1$.

As the estimators $H_k(X, Y)$, for various values of k , can be computed from a single realization of the coupled chains, this prompts the definition of a time-averaged estimator $H_{k:m}(X, Y) = (m - k + 1)^{-1} \sum_{n=k}^m H_n(X, Y)$ for integers $k \leq m$. The latter inherits the unbiasedness and finite variance properties, and can be rewritten as

$$H_{k:m}(X, Y) = M_{k:m}(X) + \sum_{n=k+1}^{\tau-1} \min\left(1, \frac{n-k}{m-k+1}\right) \{h(X_n) - h(Y_{n-1})\} \quad (2)$$

where $M_{k:m}(X) = (m - k + 1)^{-1} \sum_{n=k}^m h(X_n)$ can be viewed as the usual Markov chain estimator with m iterations and a burn-in period of $k - 1$. As before, the second term plays the role of bias correction and is equal to zero when $k \geq \tau - 1$. Hence if the value of k is sufficiently large, we can expect the variance of $H_{k:m}(X, Y)$ to be close to that of $M_{k:m}(X)$. Moreover, the cost of computing (2), which involves $\tau - 1$ applications of \bar{K} and $\max(1, m + 1 - \tau)$ applications of K , becomes comparable to m iterations under K for sufficiently large m . Therefore we can expect the asymptotic inefficiency of $H_{k:m}(X, Y)$ in the limit of our computational budget, given by the product of the expected compute cost and the variance of $H_{k:m}(X, Y)$ [Glynn and Whitt, 1992], to approach the asymptotic variance of the underlying Markov chain as m increases. We refer to Jacob et al. [2017, Section 3.1] for a more detailed discussion on the impact of k and m , and recall their proposed guideline of having k as a large quantile of the meeting time τ and m as a large multiple of k .

In practice, our proposed methodology involves simulating R pairs of coupled Markov chains $(X^{(r)}, Y^{(r)}) = (X_n^{(r)}, Y_n^{(r)})_{n \geq 0}$, $r = 1, \dots, R$ completely in parallel, with each pair taking a random compute time depending on their meeting time. As this produces R independent replicates $H_{k:m}(X^{(r)}, Y^{(r)})$, $r = 1, \dots, R$ of the unbiased estimator (2), one can compute the average $R^{-1} \sum_{r=1}^R H_{k:m}(X^{(r)}, Y^{(r)})$ to approximate $\pi(h)$. By appealing to the usual central limit theorem for independent and identically distributed random variables, confidence intervals that are justified as $R \rightarrow \infty$ can also be constructed.

Explicit constructions of coupled chains satisfying Assumptions 1–3 for Markov kernels K that are defined by Metropolis–Hastings algorithms and Gibbs samplers are given in Jacob et al. [2017, Section 4] and Jacob et al. [2018]. The focus of this article is to propose a coupling strategy that is tailored for Hamiltonian Monte Carlo chains, so as to enable the use of unbiased estimators (1)–(2). We will illustrate in Section 5 that this approach applies to realistic settings and retains the benefits of Hamiltonian Monte Carlo in terms of scaling with dimension.

2 Hamiltonian dynamics

2.1 Hamiltonian flows

Suppose that the target distribution has the form $\pi(dq) \propto \exp\{-U(q)\}dq$, where the potential function $U : \mathbb{R}^d \rightarrow \mathbb{R}_+$ satisfies the following assumptions.

Assumption 4 (Regularity and growth of potential). *The potential U is twice continuously differentiable and its gradient $\nabla U : \mathbb{R}^d \rightarrow \mathbb{R}^d$ is globally β -Lipschitz, i.e. there exists $\beta > 0$ such that $|\nabla U(q) - \nabla U(q')| \leq \beta|q - q'|$ for all $q, q' \in \mathbb{R}^d$.*

These assumptions imply at most quadratic growth of the potential, or equivalently that the tails of the target distribution are no lighter than Gaussian.

We now introduce Hamiltonian flows on the phase space $\mathbb{R}^d \times \mathbb{R}^d$, which consists of position variables $q \in \mathbb{R}^d$ and momentum variables $p \in \mathbb{R}^d$. We will be concerned with a Hamiltonian function $\mathcal{E} : \mathbb{R}^d \times \mathbb{R}^d \rightarrow \mathbb{R}_+$ of the form $\mathcal{E}(q, p) = U(q) + |p|^2/2$. We note the use of the identity mass matrix here and will rely on preconditioning in Section 5.4 to incorporate curvature properties of π . The time evolution of a particle $\{q(t), p(t)\}_{t \in \mathbb{R}_+}$ under Hamiltonian dynamics is described by the ordinary differential equations

$$\frac{d}{dt}q(t) = \nabla_p \mathcal{E}\{q(t), p(t)\} = p(t), \quad \frac{d}{dt}p(t) = -\nabla_q \mathcal{E}\{q(t), p(t)\} = -\nabla U\{q(t)\}. \quad (3)$$

Under Assumption 4, (3) with an initial condition $\{q(0), p(0)\} = (q_0, p_0) \in \mathbb{R}^d \times \mathbb{R}^d$ admits a unique solution globally on \mathbb{R}_+ [Lelièvre et al., 2010, p. 14]. Therefore the flow map $\Phi_t(q_0, p_0) = \{q(t), p(t)\}$ is well-defined for any $t \in \mathbb{R}_+$, and we will write its projection onto the position and momentum coordinates as $\Phi_t^\circ(q_0, p_0) = q(t)$ and $\Phi_t^*(q_0, p_0) = p(t)$ respectively.

It is worth recalling that Hamiltonian flows have the following properties.

Property 1 (Reversibility). *For any $t \in \mathbb{R}_+$, the inverse flow map satisfies $\Phi_t^{-1} = M \circ \Phi_t \circ M$, where $M(q, p) = (q, -p)$ denotes momentum reversal.*

Property 2 (Energy conservation). *The Hamiltonian function satisfies $\mathcal{E} \circ \Phi_t = \mathcal{E}$ for any $t \in \mathbb{R}_+$.*

Property 3 (Volume preservation). *For any $t \in \mathbb{R}_+$ and $A \in \mathcal{B}(\mathbb{R}^{2d})$, we have $\text{Leb}_{2d}\{\Phi_t(A)\} = \text{Leb}_{2d}(A)$, where Leb_{2d} denotes the Lebesgue measure on \mathbb{R}^{2d} .*

These properties imply that the extended target distribution on phase space $\tilde{\pi}(dq, dp) \propto \exp\{-\mathcal{E}(q, p)\}dqdp$ is invariant under the Markov semi-group induced by the flow, i.e. for any $t \in \mathbb{R}_+$, the pushforward measure $\Phi_t\#\tilde{\pi}$, defined as $\Phi_t\#\tilde{\pi}(A) = \tilde{\pi}\{\Phi_t^{-1}(A)\}$ for $A \in \mathcal{B}(\mathbb{R}^{2d})$, is equal to $\tilde{\pi}$.

2.2 Coupled Hamiltonian dynamics

We now consider the coupling of two particles $\{q^i(t), p^i(t)\}_{t \in \mathbb{R}_+}$, ($i = 1, 2$) evolving under (3) with initial conditions $\{q^i(0), p^i(0)\} = (q_0^i, p_0^i)$, ($i = 1, 2$). We first draw some insights from a Gaussian example.

Example 1. Let π be a Gaussian distribution on \mathbb{R} with mean $\mu \in \mathbb{R}$ and variance $\sigma^2 > 0$. In this case, we have $U(q) = (q - \mu)^2/(2\sigma^2)$, $\nabla U(q) = (q - \mu)/\sigma^2$ and the solution of (3) is

$$\Phi_t(q_0, p_0) = \begin{pmatrix} \mu + (q_0 - \mu) \cos\left(\frac{t}{\sigma}\right) + \sigma p_0 \sin\left(\frac{t}{\sigma}\right) \\ p_0 \cos\left(\frac{t}{\sigma}\right) - \frac{1}{\sigma}(q_0 - \mu) \sin\left(\frac{t}{\sigma}\right) \end{pmatrix}.$$

Hence the difference between particle positions is

$$q^1(t) - q^2(t) = (q_0^1 - q_0^2) \cos\left(\frac{t}{\sigma}\right) + \sigma(p_0^1 - p_0^2) \sin\left(\frac{t}{\sigma}\right).$$

If we set $p_0^1 = p_0^2$, then $|q^1(t) - q^2(t)| = |\cos(t/\sigma)| |q_0^1 - q_0^2|$, so for any non-negative integer n , the particles meet exactly whenever $t = (2n + 1)\pi\sigma/2$, and contraction occurs for any $t \neq \pi n\sigma$.

This example motivates a coupling that simply assigns particles the same initial momentum. Moreover, it also reveals that certain trajectory lengths will result in larger contraction than others. We now examine the utility of this approach more generally. Define $\Delta(t) = q^1(t) - q^2(t)$ as the difference between particle locations and note that

$$\frac{1}{2} \frac{d}{dt} |\Delta(t)|^2 = \Delta(t)^\top \{p^1(t) - p^2(t)\}.$$

Therefore by imposing that $p^1(0) = p^2(0)$, the function $t \mapsto |\Delta(t)|$ admits a stationary point at time $t = 0$. This is geometrically intuitive as the trajectories at time zero are parallel to one another for an infinitesimally small amount of time. To characterize this stationary point, we compute

$$\frac{1}{2} \frac{d^2}{dt^2} |\Delta(t)|^2 = -\Delta(t)^\top [\nabla U\{q^1(t)\} - \nabla U\{q^2(t)\}] + |p^1(t) - p^2(t)|^2$$

and consider the following assumption.

Assumption 5 (Local convexity of potential). *There exists a compact set $S \in \mathcal{B}(\mathbb{R}^d)$, with positive Lebesgue measure, such that the restriction of U to S is α -strongly convex, i.e. there exists $\alpha > 0$ such that $(q - q')^\top \{\nabla U(q) - \nabla U(q')\} \geq \alpha |q - q'|^2$ for all $q, q' \in S$.*

Under Assumption 5, we have

$$\frac{1}{2} \frac{d^2}{dt^2} |\Delta(0)|^2 \leq -\alpha |\Delta(0)|^2 + |p^1(0) - p^2(0)|^2$$

if $q_0^1, q_0^2 \in S$ and $q_0^1 \neq q_0^2$. Therefore by taking $p^1(0) = p^2(0)$, it follows from the second derivative test that $t = 0$ is a strict local maximum point. Continuity of $t \mapsto |\Delta(t)|^2$ implies that there exists a trajectory length $T > 0$ such that for any $t \in (0, T]$, there exists $\rho \in [0, 1)$ satisfying

$$|\Phi_t^\circ(q_0^1, p_0) - \Phi_t^\circ(q_0^2, p_0)| \leq \rho |q_0^1 - q_0^2|. \quad (4)$$

We note the dependence of T on the initial positions q_0^1, q_0^2 and momentum p_0 . We now strengthen the above claim.

Lemma 1. *Suppose that the potential U satisfies Assumptions 4–5. For any compact set $A \subset S \times S \times \mathbb{R}^d$, there exists a trajectory length $T > 0$ such that for any $t \in (0, T]$, there exists $\rho \in [0, 1)$ satisfying (4) for all $(q_0^1, q_0^2, p_0) \in A$.*

Although the qualitative result in Lemma 1 is sufficient for our purposes, we note that more quantitative results of this type have been established recently by [Mangoubi and Smith \[2017, Theorem 6\]](#) and [Bou-Rabee et al. \[2018, Theorem 2.1\]](#) to study the mixing time of Hamiltonian Monte Carlo. The preceding results show that the trajectory length T yielding contraction of the coupled system and the corresponding contraction rate ρ do not depend on d but only on the constants α and β of Assumptions 4–5. This suggests that such a coupling strategy can be effective in high dimension as long as the Hessian of U is sufficiently well-conditioned.

3 Coupled Hamiltonian Monte Carlo

3.1 Leap-frog integrator

As the flow defined by (3) is typically intractable, time discretizations are required. The leap-frog symplectic integrator is a standard choice as it preserves Properties 1 and 3. Given a step size $\varepsilon > 0$ and a number of leap-frog steps $L \in \mathbb{N}$, this scheme initializes at $(q_0, p_0) \in \mathbb{R}^d \times \mathbb{R}^d$ and iterates

$$p_{\ell+1/2} = p_\ell - \frac{\varepsilon}{2} \nabla U(q_\ell), \quad q_{\ell+1} = q_\ell + \varepsilon p_{\ell+1/2}, \quad p_{\ell+1} = p_{\ell+1/2} - \frac{\varepsilon}{2} \nabla U(q_{\ell+1}),$$

for $\ell = 0, \dots, L-1$. We write the leap-frog iteration as $\hat{\Phi}_\varepsilon(q_\ell, p_\ell) = (q_{\ell+1}, p_{\ell+1})$ and the corresponding approximation of the flow as $\hat{\Phi}_{\varepsilon, \ell}(q_0, p_0) = (q_\ell, p_\ell)$ for $\ell = 0, \dots, L$. As before, we denote by $\hat{\Phi}_{\varepsilon, \ell}^\circ(q_0, p_0) = q_\ell$ and $\hat{\Phi}_{\varepsilon, \ell}^*(q_0, p_0) = p_\ell$ the projections onto the position and momentum coordinates respectively.

It can be established that the leap-frog scheme is of order two [Hairer et al., 2005, Theorem 3.4], i.e. for sufficiently small ε , we have

$$|\hat{\Phi}_{\varepsilon, L}(q_0, p_0) - \Phi_{\varepsilon L}(q_0, p_0)| \leq C_3(q_0, p_0, L)\varepsilon^2, \quad (5)$$

$$|\mathcal{E}\{\hat{\Phi}_{\varepsilon, L}(q_0, p_0)\} - \mathcal{E}(q_0, p_0)| \leq C_4(q_0, p_0, L)\varepsilon^2, \quad (6)$$

for some positive constants C_3 and C_4 that depend continuously on the initial condition (q_0, p_0) for any number of leap-frog iterations L . To simplify our exposition and focus on the proposed methods, we will assume throughout the article that (5)–(6) hold. We refer to the book by Hairer et al. [2005] on geometric numerical integration and to the survey by Bou-Rabee and Sanz-Serna [2018] for additional assumptions under which these error bounds hold.

We now discuss how the above constants behave with dimension and integration length. Firstly, under the simplified setting of a target distribution with independent and identical marginals and appropriate growth conditions on the potential, the results of Beskos et al. [2013, Proposition 5.3 & 5.4] indicate that these constants would scale as $d^{1/2}$. Hence if we scale the step size ε as $d^{-1/4}$, advocated by Beskos et al. [2013] in this setting, we can expect these errors to be stable in high dimensions. Secondly, while the constant associated to the pathwise error bound (5) will typically grow exponentially with L [Leimkuhler and Matthews, 2015, Section 2.2.3], the constant of the Hamiltonian error bound (6) on the other hand can be stable over exponentially long time intervals εL [Hairer et al., 2005, Theorem 8.1]. Although the Hamiltonian is not conserved exactly under time discretization, one can employ a Metropolis–Hastings correction as described in the following section.

3.2 Coupled Hamiltonian Monte Carlo kernel

Hamiltonian Monte Carlo [Duane et al., 1987, Neal, 1993] is a Metropolis–Hastings algorithm that targets π using time discretized Hamiltonian dynamics as proposals. In view of Section 2.2, we consider coupling two Hamiltonian Monte Carlo chains $(Q_n^1, Q_n^2)_{n \geq 0}$ by initializing $(Q_0^1, Q_0^2) \sim \bar{\pi}_0$ and evolving the chains jointly according to the following procedure. Since the leap-frog integrator preserves Properties 1 and 3, the Metropolis–Hastings acceptance probability is

$$\alpha\{(q, p), (q', p')\} = \min[1, \exp\{\mathcal{E}(q, p) - \mathcal{E}(q', p')\}], \quad (7)$$

for $(q, p), (q', p') \in \mathbb{R}^d \times \mathbb{R}^d$. Iterating the above yields two marginal chains $(Q_n^1)_{n \geq 0}$ and $(Q_n^2)_{n \geq 0}$ that are π -invariant. Algorithm 1 amounts to running two Hamiltonian Monte Carlo chains with common random numbers; this has been considered in Neal [2002] to remove the burn-in bias, and in Mangoubi and Smith [2017] and Bou-Rabee et al. [2018] to analyze mixing properties.

Algorithm 1 Coupled Hamiltonian Monte Carlo step given (Q_{n-1}^1, Q_{n-1}^2) .

Sample momentum $P_n^* \sim \mathcal{N}(0_d, I_d)$ and $U_n \sim \mathcal{U}[0, 1]$ independently

For $i = 1, 2$

Set $(q_0^i, p_0^i) = (Q_{n-1}^i, P_n^*)$

Perform leap-frog integration to obtain $(q_L^i, p_L^i) = \hat{\Phi}_{\varepsilon, L}(q_0^i, p_0^i)$

If $U_n < \alpha\{(q_0^i, p_0^i), (q_L^i, p_L^i)\}$, set $Q_n^i = q_L^i$

Otherwise set $Q_n^i = Q_{n-1}^i$

Output (Q_n^1, Q_n^2)

We denote the associated coupled Markov transition kernel on the position coordinates as $\bar{K}_{\varepsilon, L}\{(q^1, q^2), A^1 \times A^2\}$ for $q^1, q^2 \in \mathbb{R}^d$ and $A^1, A^2 \in \mathcal{B}(\mathbb{R}^d)$. Marginally we have $\bar{K}_{\varepsilon, L}\{(q^1, q^2), A^1 \times \mathbb{R}^d\} = K_{\varepsilon, L}(q^1, A^1)$ and $\bar{K}_{\varepsilon, L}\{(q^1, q^2), \mathbb{R}^d \times A^2\} = K_{\varepsilon, L}(q^2, A^2)$, where $K_{\varepsilon, L}$ denotes the Markov transition kernel of the marginal Hamiltonian Monte Carlo chain. If we supplement Assumption 4 with the existence of a local minimum of U , then aperiodicity, Lebesgue-irreducibility and Harris recurrence of $K_{\varepsilon, L}$ follow from Durmus et al. [2017, Theorem 2]; see also Cances et al. [2007] and Livingstone et al. [2016] for previous works. Hence ergodicity follows from Meyn and Tweedie [2009, Theorem 13.0.1] and Assumption 1 is satisfied for test functions satisfying $\pi(h^{2+\kappa_1}) < \infty$ for some $\kappa_1 > 0$.

We will write the law of the coupled Hamiltonian Monte Carlo chain as $\text{pr}_{\varepsilon, L}$, and $E_{\varepsilon, L}$ to denote expectation with respect to $\text{pr}_{\varepsilon, L}$. The following result establishes that the relaxed meeting time $\tau_\delta = \inf\{n \geq 0 : |Q_n^1 - Q_n^2| \leq \delta\}$, for any $\delta > 0$, has geometric tails.

Theorem 1. *Suppose that the potential U satisfies Assumptions 4–5. Assume also that there exists $\tilde{\varepsilon} > 0$ such that for any $\varepsilon \in (0, \tilde{\varepsilon})$ and $L \in \mathbb{N}$, there exist a measurable function $V : \mathbb{R}^d \rightarrow [1, \infty)$, $\lambda \in (0, 1)$ and $b < \infty$ such that*

$$K_{\varepsilon, L}(V)(q) \leq \lambda V(q) + b \tag{8}$$

for all $q \in \mathbb{R}^d$, $\pi_0(V) < \infty$ and $\{q \in \mathbb{R}^d : V(q) \leq \ell_1\} \subseteq \{q \in S : U(q) \leq \ell_0\}$ for some $\ell_0 \in (\inf_{q \in S} U(q), \sup_{q \in S} U(q))$ and $\ell_1 > 1$ satisfying $\lambda + 2b(1 - \lambda)^{-1}(1 + \ell_1)^{-1} < 1$. Then for any $\delta > 0$, there exist $\varepsilon_0 \in (0, \tilde{\varepsilon})$ and $L_0 \in \mathbb{N}$ such that for any $\varepsilon \in (0, \varepsilon_0)$ and $L \in \mathbb{N}$ satisfying $\varepsilon L < \varepsilon_0 L_0$, we have

$$\text{pr}_{\varepsilon, L}(\tau_\delta > n) \leq C_0 \kappa_0^n \tag{9}$$

for some $C_0 \in \mathbb{R}_+$, $\kappa_0 \in (0, 1)$ and all integer $n \geq 0$.

The proof of Theorem 1 proceeds by first showing that the relaxed meeting can take place, in finite iterations, whenever both chains enter a region of the state space where the target distribution is strongly log-concave. As suggested in Neal [2002], one can expect good coupling behaviour if the chains spend enough time in this region of the state space; the second part of the proof makes this intuition precise by controlling excursions with the geometric drift condition (8). The latter can be established under additional assumptions on the potential U [Durmus et al., 2017, Theorem 9].

As Theorem 1 implies that the coupled chains can get arbitrarily close with sufficient frequency, one could potentially employ the unbiased estimation framework of Glynn and Rhee [2014] that introduces a truncation variable. To verify Assumption 2 that requires exact meetings, in the next section, we combine the coupled Hamiltonian Monte Carlo kernel with another coupled kernel that is designed to trigger exact meetings when the two chains are close.

4 Unbiased Hamiltonian Monte Carlo

4.1 Coupled random walk Metropolis–Hastings kernel

Let K_σ denote the π -invariant Gaussian random walk Metropolis–Hastings kernel with proposal covariance $\sigma^2 I_d$. The following describes a coupling of $K_\sigma(x, \cdot)$ and $K_\sigma(y, \cdot)$ that results in exact meetings with high probability when $x, y \in \mathbb{R}^d$ are close [Johnson, 1998, Jacob et al., 2017] and σ is appropriately chosen.

We begin by sampling the proposals $X^* \sim \mathcal{N}(x, \sigma^2 I_d)$ and $Y^* \sim \mathcal{N}(y, \sigma^2 I_d)$ from the maximal coupling of these two Gaussian distributions [Jacob et al., 2017, Section 4.1]. Under the maximal coupling, the probability of $\{X^* \neq Y^*\}$ is equal to the total variation distance between the distributions $\mathcal{N}(x, \sigma^2 I_d)$ and $\mathcal{N}(y, \sigma^2 I_d)$. Analytical tractability in the Gaussian case allows us to write that distance as $\text{pr}(2\sigma|Z| \leq \delta)$, where $Z \sim \mathcal{N}(0, 1)$ and $\delta = |x - y|$. By approximating the folded Gaussian cumulative distribution function [Pollard, 2005], we obtain

$$\text{pr}(X^* = Y^*) = \text{pr}(2\sigma|Z| > \delta) = 1 - (2\pi)^{-1/2} \frac{\delta}{\sigma} + \mathcal{O}\left(\frac{\delta^2}{\sigma^2}\right) \quad (10)$$

as $\delta/\sigma \rightarrow 0$. Hence to achieve $\text{pr}(X^* = Y^*) = \theta$ for some desired probability θ , σ should be chosen approximately as $\delta/\{(2\pi)^{1/2}(1-\theta)\}$.

The proposed values X^* and Y^* are then accepted according to Metropolis–Hastings acceptance probabilities, i.e. if $U^* \leq \min\{1, \pi(X^*)/\pi(x)\}$ and $U^* \leq \min\{1, \pi(Y^*)/\pi(y)\}$ respectively, where a common uniform random variable $U^* \sim \mathcal{U}[0, 1]$ is used for both chains. We denote the resulting coupled Markov transition kernel on $\{\mathbb{R}^d \times \mathbb{R}^d, \mathcal{B}(\mathbb{R}^d) \times \mathcal{B}(\mathbb{R}^d)\}$ as \bar{K}_σ . If σ is small relative to the spread of the target distribution, the probability of accepting both proposals would be high. On the other hand, (10) shows that σ needs to be large compared to δ for the event $\{X^* = Y^*\}$ to occur with high probability. This leads to a trade-off; in practice, one can monitor acceptance probabilities of random walk Metropolis–Hastings chains from preliminary runs to guide how small σ should be. Although most simulations in Section 5 will employ $\sigma = 10^{-3}$ as the default value, the sensitivity of the choice of σ on our proposed methodology will be investigated in Sections 5.3 and 5.4.

4.2 Combining coupled kernels

We now combine the coupled Hamiltonian Monte Carlo kernel $\bar{K}_{\varepsilon, L}$ with the coupled random walk Metropolis–Hastings kernel \bar{K}_σ , introduced in Sections 3.2 and 4.1 respectively, using the following mixture

$$\bar{K}_{\varepsilon, L, \sigma}\{(x, y), A \times B\} = (1 - \gamma)\bar{K}_{\varepsilon, L}\{(x, y), A \times B\} + \gamma\bar{K}_\sigma\{(x, y), A \times B\} \quad (11)$$

for $x, y \in \mathbb{R}^d$ and $A, B \in \mathcal{B}(\mathbb{R}^d)$, where $\gamma \in (0, 1)$, $\varepsilon > 0$, $L \in \mathbb{N}$, $\sigma > 0$ are appropriately chosen. The rationale for this choice is to enable exact meetings using the coupled random walk Metropolis–Hastings kernel when the chains are brought close together by the coupled Hamiltonian Monte Carlo kernel.

To address the choice of γ , in light of the efficiency considerations in Section 1.3, we should understand how γ impacts both the average meeting time, which we will investigate in Sections 5.3 and 5.4, and the asymptotic inefficiency of the marginal kernel $K_{\varepsilon, L, \sigma} = (1 - \gamma)K_{\varepsilon, L} + \gamma K_\sigma$. We now compare the asymptotic inefficiency of $K_{\varepsilon, L, \sigma}$ to that of $K_{\varepsilon, L}$. Assuming that evaluation of the potential and its gradient have the same cost, the latter is given by the product of its cost $L + 2$ and its asymptotic variance $v(h, K_{\varepsilon, L}) = \lim_{n \rightarrow \infty} \text{var}_{\varepsilon, L}\{n^{-1/2} \sum_{i=1}^n h(X_i)\}$ where $X_0 \sim \pi$ and $X_n \sim K_{\varepsilon, L}(X_{n-1}, \cdot)$ for all integer $n \geq 1$. Noting that the expected cost of $K_{\varepsilon, L, \sigma}$ is $(1 - \gamma)(L + 2) + \gamma$, we now consider its asymptotic variance $v(h, K_{\varepsilon, L, \sigma})$. By Peskun’s ordering [Peskun, 1973], we have $v(h, K_{\varepsilon, L, \sigma}) \leq v(h, P_{\varepsilon, L})$ where $P_{\varepsilon, L} = (1 - \gamma)K_{\varepsilon, L} + \gamma I$ with the

Algorithm 2 Compute unbiased estimator $H_{k:m}(X, Y)$ of $\pi(h)$

Initialize $(X_0, Y_0) \sim \bar{\pi}_0$ from a coupling with π_0 as marginals
 With probability γ , sample $X_1 \sim K_\sigma(X_0, \cdot)$; otherwise sample $X_1 \sim K_{\varepsilon,L}(X_0, \cdot)$
 Set $n = 1$. While $n < \max(m, \tau)$
 With probability γ , sample $(X_{n+1}, Y_n) \sim \bar{K}_\sigma\{(X_n, Y_{n-1}), \cdot\}$
 Otherwise sample $(X_{n+1}, Y_n) \sim \bar{K}_{\varepsilon,L}\{(X_n, Y_{n-1}), \cdot\}$
 If $X_{n+1} = Y_n$ set $\tau = n + 1$
 Increment $n \leftarrow n + 1$
 Compute $H_{k:m}(X, Y)$ using (2)

identity kernel defined as $I(x, A) = \mathbb{1}_A(x)$ for $x \in \mathbb{R}^d$ and $A \in \mathcal{B}(\mathbb{R}^d)$. We then apply [Łatuszyński and Roberts \[2013, Corollary 1\]](#) to obtain $v(h, K_{\varepsilon,L,\sigma}) \leq \gamma(1-\gamma)^{-1} \text{var}_\pi\{h(X)\} + (1-\gamma)^{-1}v(h, K_{\varepsilon,L})$. Hence in summary the relative asymptotic inefficiency can be upper bounded by

$$\{1 + \gamma(1-\gamma)^{-1}(L+2)^{-1}\} [1 + \gamma\{1 + \Psi(h, K_{\varepsilon,L})\}^{-1}], \quad (12)$$

where $\Psi(h, K_{\varepsilon,L}) = 1 + 2 \sum_{n=1}^{\infty} \text{Corr}_{\varepsilon,L}\{h(X_0), h(X_n)\}$ denotes the integrated auto-correlation time of a stationary Hamiltonian Monte Carlo chain. In view of (12), we advocate choosing only small values of γ to reduce the loss of efficiency of the marginal chain; most simulations in Section 5 will employ $\gamma = 1/20$ as the default value.

We will write $Q_\sigma(x, A) = \int_A \mathcal{N}(y; x, \sigma^2 I_d) dy$, $x \in \mathbb{R}^d$, $A \in \mathcal{B}(\mathbb{R}^d)$ as the Markov transition kernel of the Gaussian random walk, the law of the resulting coupled chain $(X_n, Y_n)_{n \geq 0}$ as $\text{pr}_{\varepsilon,L,\sigma}$, and $E_{\varepsilon,L,\sigma}$ to denote expectation with respect to $\text{pr}_{\varepsilon,L,\sigma}$. The following details the simulation of $(X_n, Y_n)_{n \geq 0}$ to compute the unbiased estimators described in Section 1.3.

The mixture kernel $K_{\varepsilon,L,\sigma}$ inherits ergodicity properties from any of its components, therefore Assumption 1 can be satisfied following the discussion in Section 3.2. Noting that the faithfulness property in Assumption 3 holds by construction, we now turn our attention to Assumption 2.

Theorem 2. *Suppose that the potential U satisfies Assumptions 4–5. Assume also that there exist $\tilde{\varepsilon} > 0$ and $\tilde{\sigma} > 0$ such that for any $\varepsilon \in (0, \tilde{\varepsilon})$, $L \in \mathbb{N}$ and $\sigma \in (0, \tilde{\sigma})$, there exist a measurable function $V : \mathbb{R}^d \rightarrow [1, \infty)$, $\lambda \in (0, 1)$, $b < \infty$ and $\mu > 0$ such that*

$$K_{\varepsilon,L}(V)(x) \leq \lambda V(x) + b \quad \text{and} \quad Q_\sigma(V)(x) \leq \mu\{V(x) + 1\} \quad (13)$$

for all $x \in \mathbb{R}^d$, $\pi_0(V) < \infty$, $\lambda_0 = (1-\gamma)\lambda + \gamma(1+\mu) < 1$ and $\{x \in \mathbb{R}^d : V(x) \leq \ell_1\} \subseteq \{x \in S : U(x) \leq \ell_0\}$ for some $\ell_0 \in (\inf_{x \in S} U(x), \sup_{x \in S} U(x))$ and $\ell_1 > 1$ satisfying $\lambda_0 + 2\{(1-\gamma)b + \gamma\mu\}(1-\lambda_0)^{-1}(1+\ell_1)^{-1} < 1$. Then there exist $\varepsilon_0 \in (0, \tilde{\varepsilon})$, $L_0 \in \mathbb{N}$ and $\sigma_0 > 0$ such that for any $\varepsilon \in (0, \varepsilon_0)$, $L \in \mathbb{N}$ satisfying $\varepsilon L < \varepsilon_0 L_0$ and $\sigma \in (0, \sigma_0)$, we have

$$\text{pr}_{\varepsilon,L,\sigma}(\tau > n) \leq C_0 \kappa_0^n \quad (14)$$

for some $C_0 \in \mathbb{R}_+$, $\kappa_0 \in (0, 1)$ and all integer $n \geq 0$.

Proof of the above result proceeds in two parts as in Theorem 1, but requires slightly stronger assumptions to ensure that the mixture kernel still satisfies a geometric drift condition. The assumptions of Theorems 1–2 can be verified for target distributions given by multivariate Gaussian distributions and posterior distributions

arising from Bayesian logistic regression; see Section E of the supplement. Although the above discussion guarantees validity of the unbiased estimator computed by Algorithm 2 for a range of tuning parameters, its efficiency will depend on the distribution of the meeting time τ induced by the coupling and mixing properties of the marginal kernel $K_{\varepsilon,L,\sigma}$.

5 Numerical illustrations

5.1 Preliminaries

In practice, we will run Algorithm 2 R times independently in parallel to obtain the unbiased estimators $H_{k:m}(X^{(r)}, Y^{(r)})$, $r = 1, \dots, R$. Following the framework of Glynn and Whitt [1992], we define the asymptotic inefficiency in the limit of our computational budget as $i(h, \bar{\pi}_0, \bar{K}_{\varepsilon,L,\sigma}) = E_{\varepsilon,L,\sigma}\{2(\tau - 1) + \max(1, m + 1 - \tau)\} \text{var}_{\varepsilon,L,\sigma}\{H_{k:m}(X, Y)\}$, assuming that applying $\bar{K}_{\varepsilon,L,\sigma}$ costs twice as much as $K_{\varepsilon,L,\sigma}$. This measure of efficiency accounts for the fact that, with a given compute budget, one can average over more estimators if each is cheaper to compute. We will approximate this inefficiency by empirical averages over the R realizations. For comparison, the asymptotic variance $v(h, K_{\varepsilon,L})$ of the standard Hamiltonian Monte Carlo estimator will be approximated with the `spectrum0.ar` function of the `coda` R package [Plummer et al., 2006] using 10,000 iterations after a burn-in of 1,000 for all examples. We will consider estimating first and second moments, i.e. set $h_i(x) = x_i$ and $h_{d+i}(x) = x_i^2$ for $i = 1, \dots, d$, and compare $i(\bar{\pi}_0, \bar{K}_{\varepsilon,L,\sigma}) = \sum_{i=1}^{2d} i(h_i, \bar{\pi}_0, \bar{K}_{\varepsilon,L,\sigma})$ with $v(K_{\varepsilon,L}) = \sum_{i=1}^{2d} v(h_i, K_{\varepsilon,L})$ at possibly different parameter configurations. An important point to be illustrated in the following is that the parameters ε and L minimizing the asymptotic inefficiency $(L + 2)v(K_{\varepsilon,L})$ might not necessarily be suitable for our proposed estimator. Lastly, we will employ the guideline of taking k as the 90% sample quantile of meeting times, obtained from a small number of preliminary runs, and setting $m = 10k$.

5.2 Toy examples

We first investigate the scalability of the proposed approach in high dimensions on a standard Gaussian target distribution on \mathbb{R}^d , by examining the average meeting time of stationary coupled chains generated by (11). For simplicity, the parameters $\sigma = 10^{-3}$ and $\gamma = 1/20$ are taken as their default values. To ensure stable acceptance probabilities as $d \rightarrow \infty$ [Beskos et al., 2013], we scale the step size as $\varepsilon = Cd^{-1/4}$ and select different constants $C > 0$ to induce a range of acceptance probabilities. The number of leap-frog steps is taken as $L = 1 + \lfloor \varepsilon^{-1} \rfloor$, which fixes the integration time εL as approximately one. For comparison, we consider (11) with $L = 1$, as this corresponds to the Metropolis-adjusted Langevin algorithm, and adopt the scaling $\varepsilon^2 = C^2 d^{-1/3}$ [Roberts and Rosenthal, 1998]; see also Section A of supplementary material for an alternative coupling. Lastly, we also consider coupled chains generated solely by the coupled random walk Metropolis–Hastings kernel described in Section 4.1, with proposal variance scaled as $\sigma^2 = C^2 d^{-1}$ [Roberts et al., 1997]. The results displayed in Fig. 1 demonstrate the effectiveness of our coupling strategy in high dimensions, and illustrates the appeal of Hamiltonian Monte Carlo kernels in high dimensional settings.

Next we consider a banana-shaped target distribution on \mathbb{R}^2 , whose potential is given by the Rosenbrock function $U(x_1, x_2) = (1 - x_1)^2 + 10(x_2 - x_1^2)^2$ for $(x_1, x_2) \in \mathbb{R}^2$. The aim here is to examine the utility of our proposed coupling for a highly non-convex potential, and to explore the use of a new coupling for Hamiltonian Monte Carlo introduced by Bou-Rabee et al. [2018, Section 2.3.2]. In contrast to Algorithm 1 which assigns the same initial momentum to both chains, the latter samples an initial momentum $P_n^1 \sim \mathcal{N}(0_d, I_d)$ for the

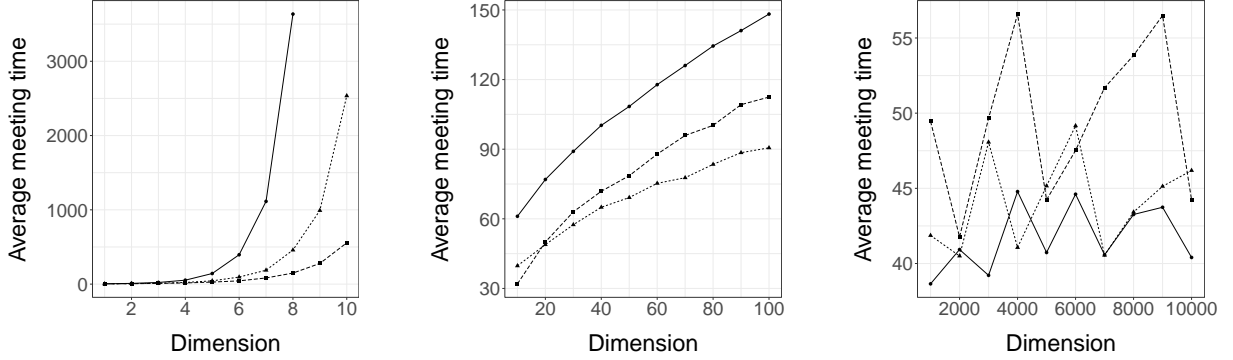


Figure 1: Gaussian example in Section 5.2. Scaling of average meeting time with dimension for 1,000 coupled chains based on random walk Metropolis–Hastings (left), Metropolis-adjusted Langevin algorithm (middle) and Hamiltonian Monte Carlo (right). The symbols and lines correspond to $C = 1$ (dot-solid), $C = 1.5$ (triangle-small dashes) and $C = 2$ (square-dashes).

first chain, and sets the initial momentum for the second chain as

$$P_n^2 = \begin{cases} P_n^1 + \kappa \Delta_{n-1}, & \text{with probability } \frac{\mathcal{N}(\bar{\Delta}_{n-1}^\top P_n^1 + \kappa |\Delta_{n-1}|; 0, 1)}{\mathcal{N}(\bar{\Delta}_{n-1}^\top P_n^1; 0, 1)}, \\ P_n^1 - 2(\bar{\Delta}_{n-1}^\top P_n^1) \bar{\Delta}_{n-1}, & \text{otherwise,} \end{cases}$$

where $\kappa > 0$ is a tuning parameter, $\Delta_{n-1} = Q_{n-1}^1 - Q_{n-1}^2$ denotes the difference between the chains at iteration $n - 1$, and $\bar{\Delta}_{n-1} = \Delta_{n-1}/|\Delta_{n-1}|$ the normalized difference. Leap-frog integration and Metropolis–Hastings acceptance of the output are then performed in the same way as Algorithm 1; the resulting coupled Hamiltonian Monte Carlo kernel is then employed in the mixture (11). We simulate 1,000 coupled chains, initialized independently from the uniform distribution on $[-5, 5]^2$, using this new coupling with $\kappa = 1$ and the previous one which corresponds to $\kappa = 0$. Employing the same parameters $(\varepsilon, L, \sigma, \gamma) = (1/500, 500, 10^{-3}, 1/20)$ for both couplings, we observe that the new coupling reduces the average meeting time from 158 to 52. This example illustrates that the proposed methodology can be used beyond convex potentials, and that alternative couplings can result in significantly shorter meeting times.

5.3 Logistic regression

We now consider a Bayesian logistic regression on the classic German credit dataset, as in Hoffman and Gelman [2014]. After including all pairwise interactions and performing standardization, the design matrix has 1,000 rows and 300 columns. Given covariates $x_i \in \mathbb{R}^{300}$, intercept $a \in \mathbb{R}$ and coefficients $b \in \mathbb{R}^{300}$, each observation $y_i \in \{0, 1\}$ is modelled as an independent Bernoulli random variable with probability of success $\{1 + \exp(-a - b^\top x_i)\}^{-1}$. The prior is specified as $a|s^2 \sim \mathcal{N}(0, s^2)$, $b|s^2 \sim \mathcal{N}(0_{300}, s^2 I_{300})$ independently, and an Exponential distribution with rate 0.01 for the variance parameter s^2 . The target π is the posterior distribution of parameters $(a, b, \log s^2)$ on \mathbb{R}^d with $d = 302$.

Initializing coupled chains independently from $\pi_0 = \mathcal{N}(0_d, I_d)$, for each parameter configuration $(\varepsilon, L) \in \{0.01, 0.0125, \dots, 0.04\} \times \{10, 20, 30\}$, we run 5 pairs of coupled Hamiltonian Monte Carlo chains for 1,000 iterations. This computation can be done independently in parallel for each configuration and repeat; the output is displayed in the left panel of Fig. 2. Although multiple configurations lead to contractive chains, it is not the case for $(\varepsilon, L) = (0.03, 10)$ which are optimal parameters for Hamiltonian Monte Carlo. For

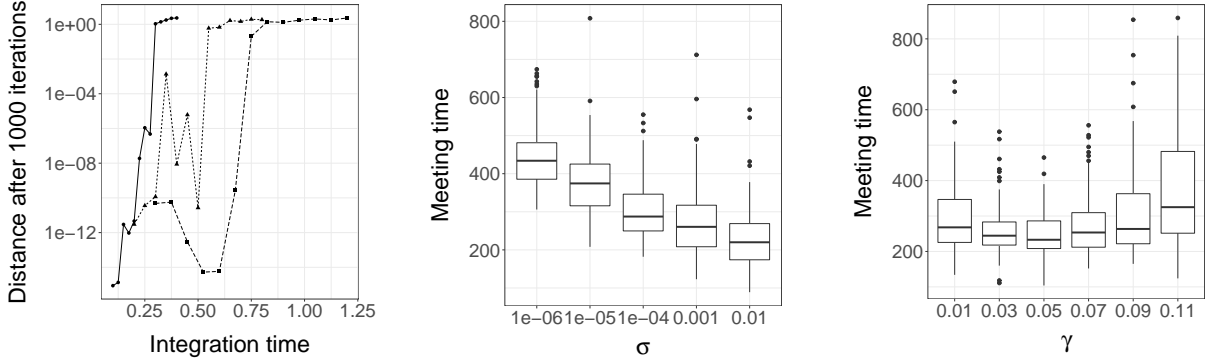


Figure 2: Logistic regression example in Section 5.3. Average distance between coupled chains at iteration 1,000 against integration time εL (left). The symbols and lines correspond to $L = 10$ (dot-solid), $L = 20$ (triangle-small dashes) and $L = 30$ (square-dashes). Boxplot of meeting times as parameter σ (middle) or γ (right) varies.

configurations that yield distances that are less than 10^{-10} , we simulate 100 meeting times in parallel using the mixture kernel (11) with $\sigma = 10^{-3}$ and $\gamma = 1/20$. We then select the parameter configuration $(\varepsilon, L) = (0.0125, 10)$ that gave the least average compute cost, taken as $L + 2$ times the average meeting time.

To illustrate the impact of σ and γ , we fix $(\varepsilon, L) = (0.0125, 10)$ and examine the distribution of meeting times as σ or γ varies. Decreasing σ leads to larger meeting times: conservatively small values of σ require more iterations before the chains get close enough for the maximal coupling to propose the same value with high probability. On the other hand, if σ was too large, large meeting times would be observed as random walk proposals would be rejected with high probability. The middle panel of Fig. 2 suggests that the effectiveness of our coupling is not highly sensitive to the choice of σ , provided that it is small enough. Similarly, the right panel of Fig. 2 also shows stable meeting times for the range of values of γ considered.

Finally, we produce $R = 1,000$ coupled chains in parallel with $(\varepsilon, L, \sigma, \gamma) = (0.0125, 10, 10^{-3}, 1/20)$ and compare the inefficiency of our estimator with the asymptotic variance of the optimal Hamiltonian Monte Carlo estimator for various choices of k and m . The results, summarized in Table 1, illustrate that bias removal comes at a cost of increased variance, and that this can be reduced with appropriate choices of k and m . Our guideline for k and m results in a relative inefficiency of 1.05 at an average compute cost of 3518 applications of $K_{\varepsilon, L, \sigma}$, or approximately 5 minutes of computing time with our implementation. Therefore, thanks to unbiasedness, we can safely average over independent copies of an estimator whose expected cost is of the order of a few thousand Hamiltonian Monte Carlo iterations.

5.4 Log-Gaussian Cox point processes

We end with a challenging high dimensional application of Bayesian inference for log-Gaussian Cox point processes on a dataset concerning the locations of 126 Scot pine saplings in a natural forest in Finland [Møller et al., 1998]. After discretizing the plot into an $n \times n$ regular grid, the number of points in each grid cell $y_i \in \mathbb{N}$ is assumed to be conditionally independent, given a latent intensity process $\Lambda_i, i \in \{1, \dots, n\}^2$, and modelled as Poisson distributed with mean $a\Lambda_i$, where $a = n^{-2}$ is the area of each grid cell. The prior is specified by $\Lambda_i = \exp(X_i)$, where $X_i, i \in \{1, \dots, n\}^2$ is a Gaussian process with mean $\mu \in \mathbb{R}$ and exponential covariance function $\Sigma_{i,j} = s^2 \exp\{-|i - j|/(nb)\}$ for $i, j \in \{1, \dots, n\}^2$. We will adopt the parameter values $s^2 = 1.91, b = 1/33$ and $\mu = \log(126) - s^2/2$ estimated by Møller et al. [1998] and infer the posterior

Table 1: Relative inefficiency of proposed estimator in logistic regression example

k	m	Cost	Variance	Relative inefficiency
1	k	436	4.0×10^2	1989.07
1	$5k$	436	3.4×10^2	1671.93
1	$10k$	436	2.8×10^2	1403.28
median(τ)	k	458	7.4×10^0	38.22
median(τ)	$5k$	1258	1.1×10^{-1}	1.58
median(τ)	$10k$	2298	4.5×10^{-2}	1.18
90% quantile(τ)	k	553	6.0×10^0	38.11
90% quantile(τ)	$5k$	1868	5.8×10^{-2}	1.23
90% quantile(τ)	$10k$	3518	2.6×10^{-2}	1.05

Cost refers to the expected compute cost, variance denotes the sum of variances when estimating first and second moments, and relative inefficiency is the ratio of the asymptotic inefficiency $i(\bar{\pi}_0, \bar{K}_{\varepsilon, L, \sigma})$ with parameters $(\varepsilon, L, \sigma, \gamma) = (0.0125, 10, 10^{-3}, 1/20)$, to the asymptotic variance $v(K_{\varepsilon, L})$ with optimal parameters $(\varepsilon, L) = (0.03, 10)$. These quantities were computed using $R = 1,000$ independent runs, while the median and 90% quantile of the meeting time were computed with 100 preliminary runs.

distribution of the latent process $X_i, i \in \{1, \dots, n\}^2$ given the count data and these hyperparameter values. We will consider three discretizations with $n \in \{16, 32, 64\}$, which correspond to target distributions π on \mathbb{R}^d with $d \in \{256, 1024, 4096\}$.

Owing to the high dimensionality of this model, the mixing of random walk Metropolis–Hastings is known to be prohibitively slow [Christensen and Waagepetersen, 2002], while the Metropolis-adjusted Langevin algorithm requires a computationally costly reparameterization to be effective [Christensen et al., 2005]. We will consider the use of Hamiltonian Monte Carlo and Riemann manifold Hamiltonian Monte Carlo with metric tensor $\Sigma^{-1} + a \exp(\mu + s^2/2)I_d$ [Girolami and Calderhead, 2011]. We proceed as in Section 5.3 to seek parameter configurations $(\varepsilon, L) \in \{0.05, 0.07, \dots, 0.45\} \times \{10, 20, 30\}$ that yield contractive coupled chains with small compute cost, when initialized independently from the prior distribution. Although both algorithms have multiple configurations that result in contractive chains, the parameters ε and L that were optimal for these methods only led to contractive coupled Riemann manifold Hamiltonian Monte Carlo chains for all three discretizations. By simulating 100 meeting times with $\sigma = 10^{-3}$ and $\gamma = 1/20$ for configurations that yield distances of less than 10^{-10} , for $d \in \{256, 1024, 4096\}$ respectively, we select $(\varepsilon, L) \in \{(0.11, 10), (0.15, 10), (0.17, 10)\}$ for Hamiltonian Monte Carlo, and $(\varepsilon, L) \in \{(0.11, 10), (0.11, 10), (0.13, 10)\}$ for Riemann manifold Hamiltonian Monte Carlo, which gave the smallest average compute cost for each algorithm. The corresponding meeting times in the left panel of Fig. 3 show the effectiveness of our coupling strategy even in high dimensions. The middle and right panels of Fig. 3, which display the meeting times of coupled Riemann manifold Hamiltonian Monte Carlo chains for the finest discretization, also illustrate the robustness of our coupling to the choice of σ and γ .

With the above parameters and the guideline for choosing k and m , we computed $R = 1,000$ coupled chains in parallel for each algorithm and discretization. For $d \in \{256, 1024, 4096\}$ respectively, the relative inefficiency was found to be 11.00, 5.43, 2.73 for Hamiltonian Monte Carlo, and 11.68, 7.85, 3.72 for Riemann manifold Hamiltonian Monte Carlo. For the finest discretization, the average compute time was approximately 90 and 20 minutes with our implementation. Despite some loss of efficiency, the benefits of exploiting

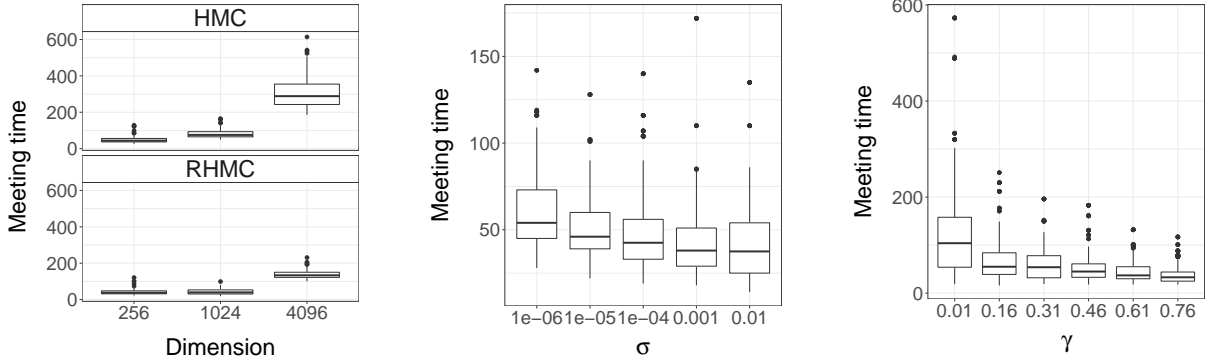


Figure 3: Cox process example in Section 5.4. Boxplot of meeting times for both algorithms and all three discretizations (left), and as parameter σ (middle) or γ (right) varies.

parallel computation for this problem is apparent since one can only run 4439 and 714 iterations of these algorithms respectively for the same compute time.

6 Discussion

Construction of couplings could be explored for other variants of the Hamiltonian Monte Carlo method, such as the use of partial momentum refreshment [Horowitz, 1991], the adaptation of tuning parameters [Hoffman and Gelman, 2014], different choices of kinetic energy [Livingstone et al., 2017], and in combination with new sampling paradigms [Pollock et al., 2016, Fearnhead et al., 2018, Vanetti et al., 2017]. Other ways of leveraging parallel hardware for Hamiltonian Monte Carlo include the work in Calderhead [2014], which builds on Tjelmeland [2004] and focuses on parallel computation at each iteration of the algorithm.

Acknowledgement

The computations in this article were run on the Odyssey cluster supported by the FAS Division of Science, Research Computing Group at Harvard University. Pierre E. Jacob gratefully acknowledges support by the National Science Foundation through grant DMS-1712872. Both authors gratefully acknowledge support by the Army Research Office through grant W911NF-15-1-0172.

Supplementary material

An R package is available at github.com/pierrejacob/debiasedhmc and contains the scripts used to produce the figures of this article. The supplementary material (available below) includes an alternative coupling for the Metropolis-adjusted Langevin algorithm, additional simulation results on truncated Gaussian distributions, the proofs of Lemma 1 and Theorems 1–2, and notes on verifying the assumptions of Theorems 1–2 for target distributions given by posterior distributions of Bayesian logistic regression.

References

- A. Beskos, N. Pillai, G. Roberts, J. M. Sanz-Serna, and A. Stuart. Optimal tuning of the Hybrid Monte Carlo algorithm. *Bernoulli*, 19(5A):1501–1534, 2013. [1](#), [6](#), [10](#)
- M. Betancourt. A conceptual introduction to Hamiltonian Monte Carlo. *arXiv preprint arXiv:1701.02434*, 2017. [1](#)
- M. Betancourt, S. Byrne, S. Livingstone, and M. Girolami. The geometric foundations of Hamiltonian Monte Carlo. *Bernoulli*, 23(4A):2257–2298, 2017. [1](#)
- N. Bou-Rabee and J. M. Sanz-Serna. Geometric integrators and the Hamiltonian Monte Carlo method. *Acta Numerica*, 27:113–206, 2018. [6](#)
- N. Bou-Rabee, A. Eberle, and R. Zimmer. Coupling and convergence for Hamiltonian Monte Carlo. *arXiv preprint arXiv:1805.00452*, 2018. [1](#), [5](#), [6](#), [10](#)
- S. P. Brooks, A. Gelman, G. Jones, and X. L. Meng. *Handbook of Markov chain Monte Carlo*. CRC press, 2011. [1](#)
- B. Calderhead. A general construction for parallelizing Metropolis–Hastings algorithms. *Proceedings of the National Academy of Sciences*, 111(49):17408–17413, 2014. [14](#)
- E. Cancès, F. Legoll, and G. Stoltz. Theoretical and numerical comparison of some sampling methods for molecular dynamics. *ESAIM: Mathematical Modelling and Numerical Analysis*, 41(2):351–389, 2007. [7](#)
- B. Carpenter, A. Gelman, M. D. Hoffman, D. Lee, B. Goodrich, M. Betancourt, M. A. Brubaker, J. Guo, P. Li, and A. Riddell. Stan: a probabilistic programming language. *Journal of Statistical Software*, 20:1–37, 2016. [1](#)
- G. Casella, M. Lavine, and C. P. Robert. Explaining the perfect sampler. *The American Statistician*, 55(4):299–305, 2001. [1](#)
- O. F. Christensen and R. Waagepetersen. Bayesian prediction of spatial count data using generalized linear mixed models. *Biometrics*, 58(2):280–286, 2002. [13](#)
- O. F. Christensen, G. O. Roberts, and J. S. Rosenthal. Scaling limits for the transient phase of local Metropolis–Hastings algorithms. *J. Royal Statist. Society Series B*, 67(2):253–268, 2005. [13](#)
- A. S. Dalalyan. Theoretical guarantees for approximate sampling from smooth and log-concave densities. *J. Royal Statist. Society Series B*, 79(3):651–676, 2017a. [23](#)
- A. S. Dalalyan. Further and stronger analogy between sampling and optimization: Langevin Monte Carlo and gradient descent. In *Proceedings of the 2017 Conference on Learning Theory*, volume 65 of *Proceedings of Machine Learning Research*, pages 678–689. PMLR, 07–10 Jul 2017b. URL <http://proceedings.mlr.press/v65/dalalyan17a.html>. [17](#)
- S. Duane, A. D. Kennedy, B. J. Pendleton, and D. Roweth. Hybrid Monte Carlo. *Physics Letters B*, 195(2):216–222, 1987. [1](#), [6](#)
- A. Durmus, E. Moulines, and E. Saksman. On the convergence of Hamiltonian Monte Carlo. *arXiv preprint arXiv:1705.00166*, 2017. [1](#), [7](#), [24](#), [25](#)
- P. Fearnhead, J. Bierkens, M. Pollock, and G. O. Roberts. Piecewise deterministic Markov processes for continuous-time Monte Carlo. *Statist. Science*, 33(3):386–412, 2018. [14](#)
- M. Girolami and B. Calderhead. Riemann manifold Langevin and Hamiltonian Monte Carlo methods. *J. Royal Statist. Society Series B*, 73(2):123–214, 2011. [2](#), [13](#)
- P. W. Glynn and P. Heidelberger. Analysis of parallel replicated simulations under a completion time constraint. *ACM Transactions on Modeling and Computer Simulations*, 1(1):3–23, 1991. [2](#)
- P. W. Glynn and C.-H. Rhee. Exact estimation for Markov chain equilibrium expectations. *Journal of Applied Probability*, 51(A):377–389, 2014. [2](#), [7](#)

- P. W. Glynn and W. Whitt. The asymptotic efficiency of simulation estimators. *Operations Research*, 40(3): 505–520, 1992. 3, 10
- E. Hairer, G. Wanner, and C. Lubich. *Geometric numerical integration: structure-preserving algorithms for ordinary differential equations*. Springer-Verlag, New York, 2005. 6
- M. D. Hoffman and A. Gelman. The No-U-Turn Sampler: adaptively setting path lengths in Hamiltonian Monte Carlo. *Journal of Machine Learning Research*, 15(1):1593–1623, 2014. 1, 11, 14
- A. M. Horowitz. A generalized guided Monte Carlo algorithm. *Physics Letters B*, 268(2):247–252, 1991. 14
- M. Huber. *Perfect simulation*, volume 148. CRC Press, 2016. 1
- P. E. Jacob, J. O’Leary, and Y. F. Atchadé. Unbiased Markov chain Monte Carlo with couplings. *arXiv preprint arXiv:1708.03625v2*, 2017. 2, 3, 8, 21
- P. E. Jacob, F. Lindsten, and T. B. Schön. Smoothing with couplings of conditional particle filters. *J. American Statist. Assoc.*, 2018. 3
- V. E. Johnson. A coupling-regeneration scheme for diagnosing convergence in Markov chain Monte Carlo algorithms. *J. American Statist. Assoc.*, 93(441):238–248, 1998. 8
- K. Łatuszyński and G. O. Roberts. CLTs and asymptotic variance of time-sampled Markov chains. *Methodology and Computing in Applied Probability*, 15(1):237–247, 2013. 9
- B. Leimkuhler and C. Matthews. *Molecular Dynamics*. Springer-Verlag, New York, 2015. 6
- T. Lelièvre, M. Rousset, and G. Stoltz. *Free Energy Computations: A Mathematical Perspective*. Imperial College Press, 2010. ISBN 978-1-84816-248-8. 1, 4
- S. Livingstone, M. Betancourt, S. Byrne, and M. Girolami. On the geometric ergodicity of Hamiltonian Monte Carlo. *arXiv preprint arXiv:1601.08057*, 2016. 1, 7
- S. Livingstone, M. F. Faulkner, and G. O. Roberts. Kinetic energy choice in Hamiltonian/hybrid Monte Carlo. *arXiv preprint arXiv:1706.02649*, 2017. 14
- O. Mangoubi and A. Smith. Rapid mixing of Hamiltonian Monte Carlo on strongly log-concave distributions. *arXiv preprint arXiv:1708.07114*, 2017. 1, 5, 6
- S. Meyn and R. Tweedie. *Markov chains and stochastic stability*. Cambridge University Press, 2nd edition, 2009. 7
- J. Møller, A. R. Syversveen, and R. P. Waagepetersen. Log Gaussian Cox processes. *Scandinavian Journal of Statistics*, 25(3):451–482, 1998. 12
- P. Mykland, L. Tierney, and B. Yu. Regeneration in Markov chain samplers. *J. American Statist. Assoc.*, 90(429):233–241, 1995. 2
- R. M. Neal. Bayesian learning via stochastic dynamics. Advances in neural information processing systems, pages 475–475, 1993. 1, 6
- R. M. Neal. Circularly-coupled Markov chain sampling. *arXiv preprint arXiv:1711.04399*, 2002. 2, 6, 7
- A. Pakman. tmg: truncated multivariate Gaussian sampling. *CRAN*, 2012. URL <https://cran.r-project.org/package=tmg>. 17
- A. Pakman and L. Paninski. Exact Hamiltonian Monte Carlo for truncated multivariate Gaussians. *Journal of Computational and Graphical Statistics*, 23(2):518–542, 2014. 17, 18
- P. H. Peskun. Optimum Monte-Carlo sampling using Markov chains. *Biometrika*, 60(3):607–612, 1973. 8
- M. Plummer, N. Best, K. Cowles, and K. Vines. CODA: Convergence diagnosis and output analysis for MCMC. *R News*, 6(1):7–11, 2006. URL <https://journal.r-project.org/archive/>. 10
- D. Pollard. *Chapter 3: Total variation distance between measures*. Asymptopia, 2005. URL <http://www.stat.yale.edu/~pollard/Courses/607.spring05/handouts/Totalvar.pdf>. 8
- M. Pollock, P. Fearnhead, A. M. Johansen, and G. O. Roberts. The scalable Langevin exact algorithm: Bayesian inference for big data. *arXiv preprint arXiv:1609.03436*, 2016. 14

- G. O. Roberts and J. S. Rosenthal. Optimal scaling of discrete approximations to Langevin diffusions. *J. Royal Statist. Society Series B*, 60(1):255–268, 1998. [10](#)
- G. O. Roberts, A. Gelman, and W. R. Gilks. Weak convergence and optimal scaling of random walk Metropolis algorithms. *Ann. Applied Probability*, 7(1):110–120, 1997. [10](#)
- J. S. Rosenthal. Faithful couplings of Markov chains: now equals forever. *Advances in Applied Mathematics*, 18(3):372–381, 1997. ISSN 0196-8858. [3](#)
- J. S. Rosenthal. Parallel computing and Monte Carlo algorithms. *Far East Journal of Theoretical Statistics*, 4(2):207–236, 2000. [1](#)
- H. Tjelmeland. Using all Metropolis–Hastings proposals to estimate mean values. Technical report, Department of Mathematical Sciences, Norwegian University of Science and Technology, 2004. [14](#)
- P. Vanetti, A. Bouchard-Côté, G. Deligiannidis, and A. Doucet. Piecewise deterministic Markov chain Monte Carlo. *arXiv preprint arXiv:1707.05296*, 2017. [14](#)

A Coupling Metropolis-adjusted Langevin algorithm

We present an alternative to the construction in (11) for the case $L = 1$, which reduces to the Metropolis-adjusted Langevin algorithm with step size $\varepsilon^2 > 0$. In this case, the coupled Hamiltonian Monte Carlo kernel $\bar{K}_{\varepsilon,1}$, introduced in Section 3, corresponds to a synchronous coupling of the proposal transition kernel $Q_\varepsilon(x, A) = \int_A \mathcal{N}\{y; x + \varepsilon^2 \nabla \log \pi(x)/2, \varepsilon^2 I_d\} dy$, $x \in \mathbb{R}^d$, $A \in \mathcal{B}(\mathbb{R}^d)$, associated to the Euler–Maruyama discretization of a π -invariant Langevin diffusion on \mathbb{R}^d [Dalalyan, 2017b].

To construct a coupling of $K_{\varepsilon,1}(x, \cdot)$ and $K_{\varepsilon,1}(y, \cdot)$ that prompts exact meetings when $x, y \in \mathbb{R}^d$ are close, we can sample the proposals (X^*, Y^*) from the maximal coupling of $Q_\varepsilon(x, \cdot)$ and $Q_\varepsilon(y, \cdot)$. Writing $\delta = |x - y|$, it follows from Assumption 4 and the approximation in (10) that

$$\text{pr}(X^* = Y^*) \geq 1 - \frac{(2 + \beta\varepsilon^2) \delta}{2(2\pi)^{1/2} \varepsilon} + \mathcal{O}\left(\frac{\delta^2}{\varepsilon^2}\right)$$

as $\delta/\varepsilon \rightarrow 0$. As in Section 4.1, the proposed values are then accepted with Metropolis–Hastings acceptance probabilities with a common uniform random variable for both chains. We denote the resulting coupled Markov transition kernel on $\{\mathbb{R}^d \times \mathbb{R}^d, \mathcal{B}(\mathbb{R}^d) \times \mathcal{B}(\mathbb{R}^d)\}$ as \bar{K}_ε . For some pre-specified threshold $\delta_0 > 0$, we can combine these coupled kernels by considering

$$\bar{K}\{(x, y), A \times B\} = \mathbb{1}_{D_{\delta_0}^c}(x, y) \bar{K}_{\varepsilon,1}\{(x, y), A \times B\} + \mathbb{1}_{D_{\delta_0}}(x, y) \bar{K}_\varepsilon\{(x, y), A \times B\}$$

for $x, y \in \mathbb{R}^d$ and $A, B \in \mathcal{B}(\mathbb{R}^d)$, where $D_{\delta_0} = \{(x, y) \in \mathbb{R}^d \times \mathbb{R}^d : |x - y| \leq \delta_0\}$ and $D_{\delta_0}^c = \mathbb{R}^d \times \mathbb{R}^d \setminus D_{\delta_0}$. This coupled kernel admits the marginal Metropolis-adjusted Langevin algorithm kernel $K_{\varepsilon,1}$ as marginals, i.e. $\bar{K}\{(x, y), A \times \mathbb{R}^d\} = K_{\varepsilon,1}(x, A)$ and $\bar{K}\{(x, y), \mathbb{R}^d \times A\} = K_{\varepsilon,1}(y, A)$ for all $x, y \in \mathbb{R}^d$ and $A \in \mathcal{B}(\mathbb{R}^d)$, as this holds for both $\bar{K}_{\varepsilon,1}$ and \bar{K}_ε .

B Truncated Gaussian distribution

We investigate coupling Hamiltonian Monte Carlo on truncated Gaussian distributions constrained by quadratic inequalities. Pakman and Paninski [2014] introduced an algorithm that generates trajectories which undergo exact Hamiltonian dynamics and bounce off the constraints. Implementing our method only involved simple modifications of their `tmg` R package [Pakman, 2012].

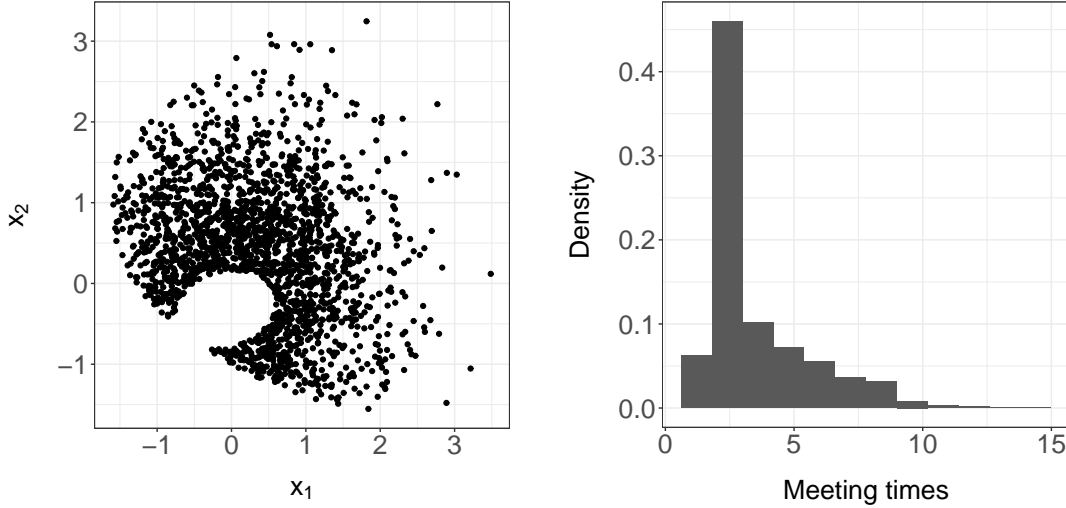


Figure 4: Truncated Gaussian example in Section B. Scatter plot of 2,000 Hamiltonian Monte Carlo samples approximating a Gaussian distribution truncated by quadratic constraints (left). Histogram of relaxed meeting times for 1,000 coupled Hamiltonian Monte Carlo chains (right).

Following Pakman and Paninski [2014], we consider a bivariate standard Gaussian distribution restricted to the set $\{(x_1, x_2) \in \mathbb{R}^2 : (x_1 - 4)^2/32 + (x_2 - 1)^2/8 \leq 1, 4x_1^2 + 8x_2^2 - 2x_1x_2 + 5x_2 \geq 1\}$ and use $\pi/2$ as the trajectory length, as advocated in Pakman and Paninski [2014]. The left panel of Fig. 4 displays 2,000 Hamiltonian Monte Carlo samples. Setting $(2, 0)$ as the initial position of both chains, the coupling proposed in Section 2.2 yields rapidly contracting chains that are within machine precision in a few iterations. A histogram of relaxed meeting times, with respect to machine precision, is shown in the right panel of Fig. 4. Our guideline for the choice of k and m yields $k = 6$ and $m = 60$, based on 100 draws of meeting times. With these values, we computed $R = 1,000$ unbiased estimators and obtained an approximate asymptotic inefficiency of 7.15. In this case, the loss of efficiency is insignificant compared to the Hamiltonian Monte Carlo algorithm, for which the asymptotic variance was found to be approximately 6.41.

C Intermediate results

Proof of Lemma 1. Take $(q_0^1, q_0^2, p_0) \in A$. Applying Taylor’s theorem on $\Delta(t)$ around $t = 0$ gives

$$\Delta(t) = \Delta(0) - \frac{1}{2}t^2G_0 - \frac{1}{6}t^3G_*$$

for some $t_* \in (0, t)$, where $G_0 = \nabla U(q_0^1) - \nabla U(q_0^2)$ and

$$G_* = \nabla^2 U\{q^1(t_*)\}p^1(t_*) - \nabla^2 U\{q^2(t_*)\}p^2(t_*).$$

We will control each term of the expansion

$$|\Delta(t)|^2 = |\Delta(0)|^2 - t^2\Delta(0)^\top G_0 - \frac{1}{3}t^3\Delta(0)^\top G_* + \frac{1}{4}t^4|G_0|^2 + \frac{1}{6}t^5G_0^\top G_* + \frac{1}{36}t^6|G_*|^2.$$

Using strong convexity, the Lipschitz assumption and Young’s inequality

$$|\Delta(t)|^2 \leq \left(1 - \alpha t^2 + \frac{1}{6}t^3 + \frac{1}{4}\beta^2 t^4 + \frac{1}{12}\beta^2 t^5\right) |\Delta(0)|^2 + \left(\frac{1}{6}t^3 + \frac{1}{12}t^5 + \frac{1}{36}t^6\right) |G_*|^2.$$

By Young's inequality and the Lipschitz assumption

$$\begin{aligned}
|G_*|^2 &\leq 2\|\nabla^2 U\{q^1(t_*)\}\|_2^2 |p^1(t_*)|^2 + 2\|\nabla^2 U\{q^2(t_*)\}\|_2^2 |p^2(t_*)|^2 \\
&\leq 2\beta^2 \{|\Phi_{t_*}^*(q_0^1, p_0)|^2 + |\Phi_{t_*}^*(q_0^2, p_0)|^2\} \\
&\leq 2\beta^2 \sup_{(q_0^1, q_0^2, p_0) \in A} \{|\Phi_{t_*}^*(q_0^1, p_0)|^2 + |\Phi_{t_*}^*(q_0^2, p_0)|^2\}
\end{aligned}$$

where $\|\cdot\|_2$ denotes the spectral norm. The above supremum is attained by continuity of the mapping $(q, p) \mapsto \Phi_{t_*}^*(q, p)$. The claim (4) follows by combining both inequalities and taking t sufficiently small. \square

As noted by an anonymous reviewer, inspection of the proof of Lemma 1 reveals that one can relax local strong convexity in Assumption 5 to the condition

$$(q - q')^\top \{\nabla U(q) - \nabla U(q')\} \geq f(|q - q'|) \quad (15)$$

for all $q, q' \in S$, where $f : \mathbb{R}_+ \rightarrow \mathbb{R}_+$ is a function satisfying $f(x) > 0$ whenever $x > 0$ and $f(x) \geq Cx^2$ for some $C > 0$ and all $x \in \mathbb{R}_+$. We now concern ourselves with an interpretation of (15). We shall assume in the following that S contains a local mode, i.e. there exists $q^* \in S$ such that $\nabla U(q^*) = 0$. It can be shown that strong convexity on S is equivalent to

$$U(q) \geq U(q') + (q - q')^\top \nabla U(q') + \frac{\alpha}{2} |q - q'|^2 \quad (16)$$

for all $q, q' \in S$. This implies $U(q) \geq U(q^*) + \alpha|q - q^*|^2/2$ for all $q \in S$, which can be seen as having the ratio of the target density and the Gaussian density $q \mapsto \mathcal{N}(q; q^*, \alpha^{-1}I_d)$ being upper bounded on S .

Suppose additionally that S is convex and f is homogeneous of degree $k \in \mathbb{N}$, i.e. $f(cx) = c^k f(x)$ for all $c \in \mathbb{R}_+$ and $x \in \mathbb{R}_+$. Fix $q, q' \in S$ and define the function $g(c) = U\{q' + c(q - q')\}$ for $c \in [0, 1]$. We will write its derivative as $g'(c) = (q - q')^\top \nabla U\{q' + c(q - q')\}$. Applying (15) and homogeneity of f gives $g'(c) \geq g'(0) + c^{k-1} f(|q - q'|)$. By continuity of ∇U and fundamental theorem of calculus

$$\begin{aligned}
U(q) = g(1) &= g(0) + \int_0^1 g'(c) dc \geq g(0) + g'(0) + f(|q - q'|) \int_0^1 c^{k-1} dc \\
&\geq U(q') + (q - q')^\top \nabla U(q') + \frac{1}{k} f(|q - q'|)
\end{aligned} \quad (17)$$

for all $q, q' \in S$. Therefore this implies that the ratio of the target density and the function $q \mapsto \exp\{-f(|q - q^*|)/k\}$ is upper bounded on S . Note also that (17) only implies $(q - q')^\top \{\nabla U(q) - \nabla U(q')\} \geq (2/k)f(|q - q'|)$ for all $q, q' \in S$, so (15) and (17) are only equivalent when $k = 2$. This completes our discussion of (15).

To prove Theorem 1, we first establish the following intermediate result. For any measurable function $f : \Omega \rightarrow \mathbb{R}$ and subset $A \subseteq \Omega$, we will write its level sets as $L_\ell(f) = \{x \in \Omega : f(x) \leq \ell\}$ for $\ell \in \mathbb{R}$ and its restriction to A as $f_A : A \rightarrow \mathbb{R}$.

Proposition 1. *Suppose that the potential U satisfies Assumptions 4–5. Then for any $\delta > 0$, $u_0 > \inf_{q \in S} U(q)$ and $u_1 < \sup_{q \in S} U(q)$ with $u_0 < u_1$, there exist $\bar{\varepsilon} > 0$ and $\bar{L} \in \mathbb{N}$ such that for any $\varepsilon \in (0, \bar{\varepsilon})$ and $L \in \mathbb{N}$ satisfying $\varepsilon L < \bar{\varepsilon} \bar{L}$, there exist $v_0 \in (u_0, u_1)$, $n_0 \in \mathbb{N}$ and $\omega \in (0, 1)$ such that*

$$\inf_{q^1, q^2 \in S_0} \bar{K}_{\varepsilon, L}^{n_0} \{(q^1, q^2), D_\delta\} \geq \omega, \quad (18)$$

where $S_0 = L_{v_0}(U_S)$ is compact with positive Lebesgue measure,

$$\bar{K}_{\varepsilon, L}^n \{(q^1, q^2), A^1 \times A^2\} = \text{pr}_{\varepsilon, L} \{(Q_n^1, Q_n^2) \in A^1 \times A^2 \mid (Q_0^1, Q_0^2) = (q^1, q^2)\}$$

denotes the n -step transition probabilities of the coupled chain, and $D_\delta = \{(q, q') \in \mathbb{R}^d \times \mathbb{R}^d : |q - q'| \leq \delta\}$.

Proof of Proposition 1. Suppose that the chains $(Q_n^1)_{n \geq 0}, (Q_n^2)_{n \geq 0}$ are initialized at $Q_0^1 = q^1 \in S$ and $Q_0^2 = q^2 \in S$. Let $K(p) = |p|^2/2$ denote the kinetic energy function. By compactness of $A = S \times S \times L_{k_0}(K)$, for some $k_0 > 0$ to be specified, it follows from Lemma 1 that there exists a trajectory length $T > 0$ such that for any $t \in (0, T]$, there exists $\rho_0 \in [0, 1)$ satisfying

$$|\Phi_t^\circ(Q_0^1, P_1^*) - \Phi_t^\circ(Q_0^2, P_1^*)| \leq \rho_0 |Q_0^1 - Q_0^2|$$

for all $(Q_0^1, Q_0^2, P_1^*) \in A$. Considering a fixed integration time $t \in (0, T]$, there exists $\omega_1 \in (0, 1)$ such that for any $\varepsilon > 0$ and $L \in \mathbb{N}$

$$\text{pr}_{\varepsilon, L} \left\{ |\Phi_t^\circ(Q_0^1, P_1^*) - \Phi_t^\circ(Q_0^2, P_1^*)| \leq \rho_0 |Q_0^1 - Q_0^2| \mid (Q_0^1, Q_0^2) = (q^1, q^2) \right\} \geq \omega_1.$$

By the triangle inequality, the pathwise error bound of the leap-frog integrator (5) and compactness of A , there exist $\varepsilon_1 > 0$ and $\rho_1 \in [0, 1)$ such that

$$\text{pr}_{\varepsilon, L} \left\{ |\hat{\Phi}_{\varepsilon, L}^\circ(Q_0^1, P_1^*) - \hat{\Phi}_{\varepsilon, L}^\circ(Q_0^2, P_1^*)| \leq \rho_1 |Q_0^1 - Q_0^2| \mid (Q_0^1, Q_0^2) = (q^1, q^2) \right\} \geq \omega_1$$

for $\varepsilon \in (0, \varepsilon_1)$ and $L \in \mathbb{N}$ satisfying $\varepsilon L = t$. Using the Hamiltonian error bound of the leap-frog integrator (6) and compactness of A , it follows from (7) that there exist $\varepsilon_2 \in (0, \varepsilon_1]$ and $\omega_2 \in (0, \omega_1)$ such that

$$\text{pr}_{\varepsilon, L} \left\{ Q_1^1 = \hat{\Phi}_{\varepsilon, L}^\circ(Q_0^1, P_1^*), Q_1^2 = \hat{\Phi}_{\varepsilon, L}^\circ(Q_0^2, P_1^*) \mid (Q_0^1, Q_0^2) = (q^1, q^2) \right\} \geq 1 - \omega_2$$

for $\varepsilon \in (0, \varepsilon_2)$ and $L \in \mathbb{N}$ satisfying $\varepsilon L = t$. Noting that

$$\begin{aligned} \left\{ |Q_1^1 - Q_1^2| \leq \rho_1 |Q_0^1 - Q_0^2| \right\} \supseteq & \left\{ |\hat{\Phi}_{\varepsilon, L}^\circ(Q_0^1, P_1^*) - \hat{\Phi}_{\varepsilon, L}^\circ(Q_0^2, P_1^*)| \leq \rho_1 |Q_0^1 - Q_0^2| \right\} \\ & \cap \left\{ Q_1^1 = \hat{\Phi}_{\varepsilon, L}^\circ(Q_0^1, P_1^*), Q_1^2 = \hat{\Phi}_{\varepsilon, L}^\circ(Q_0^2, P_1^*) \right\}, \end{aligned}$$

by Fréchet's inequality

$$\inf_{q^1, q^2 \in S} \text{pr}_{\varepsilon, L} \left\{ |Q_1^1 - Q_1^2| \leq \rho_1 |Q_0^1 - Q_0^2| \mid (Q_0^1, Q_0^2) = (q^1, q^2) \right\} \geq \omega_1 - \omega_2 > 0. \quad (19)$$

Consider $\delta > 0$, $u_0 > \inf_{q \in S} U(q)$ and $u_1 < \sup_{q \in S} U(q)$ with $u_0 < u_1$, and define the sets $A_\ell = L_\ell(U_S) \times L_{u_1 - \ell}(K) \subset L_{u_1}(\mathcal{E})$ for $\ell \in (u_0, u_1)$. As continuity and convexity of U_S imply that it is a closed function, its level sets $L_\ell(U_S)$ for $\ell \in (u_0, u_1)$ are closed. Moreover, under the assumptions on U and S , it follows that these level sets are compact with positive Lebesgue measure. To iterate the argument in (19), note first that if $(q, p) \in A_\ell$, Property 2 and continuity of U and the mapping $t \mapsto \Phi_t^\circ(q, p)$ imply that $\Phi_t^\circ(q, p) \in L_{u_1}(U_S)$ for any $t \in \mathbb{R}_+$. Due to time discretization, we can only conclude using (6) and compactness of A_ℓ that there exists $\eta_0 > 0$ such that $\hat{\Phi}_{\varepsilon, L}^\circ(q, p) \in L_{u_1 + \eta_0}(U)$ for all $(q, p) \in A_\ell$. Set $n_0 = \inf \{ n \geq 1 : \rho_1^n \sup_{q, q' \in S} |q - q'| \leq \delta \}$ and take $v_0 \in (u_0, u_1), k_0 > 0, \eta_0 > 0$ small enough such that $v_0 + (n_0 + 1)k_0 + n_0\eta_0 < u_1$ holds. Then we can conclude that

$$\inf_{q^1, q^2 \in L_{v_0}(U_S)} \text{pr}_{\varepsilon, L} \left\{ |Q_{n_0}^1 - Q_{n_0}^2| \leq \delta \mid (Q_0^1, Q_0^2) = (q^1, q^2) \right\} \geq (\omega_1 - \omega_2)^{n_0} > 0$$

and (18) follows. \square

D Proofs of Theorems 1 and 2

Proof of Theorem 1. For any $\delta > 0$, we can apply Proposition 1 with $u_0 = \ell_0$ and any $u_1 \in (\ell_0, \sup_{q \in S} U(q))$; the following adopts the notation in the conclusion of Proposition 1. This proof follows the arguments in

Jacob et al. [2017, Proposition 3.4] with modifications to suit our setup. For $\varepsilon \in (0, \min\{\bar{\varepsilon}, \bar{\varepsilon}\})$ and $L \in \mathbb{N}$ satisfying $\varepsilon L < \bar{\varepsilon} \bar{L}$, it follows from assumption (8) that the coupled transition kernel $\bar{K}_{\varepsilon, L}$ satisfies the geometric drift condition

$$\bar{K}_{\varepsilon, L}(\bar{V})(q, q') \leq \lambda \bar{V}(q, q') + b$$

for all $q, q' \in \mathbb{R}^d$ with $\bar{V}(q, q') = \{V(q) + V(q')\}/2$ as the bivariate Lyapunov function. Iterating gives $\bar{K}_{\varepsilon, L}^{n_0}(\bar{V})(q, q') \leq \lambda^{n_0} \bar{V}(q, q') + b/(1 - \lambda)$. For $(q, q') \notin L_{\ell_0}(U_S) \times L_{\ell_0}(U_S)$ which implies $(q, q') \notin L_{\ell_1}(V) \times L_{\ell_1}(V)$, we have $\bar{V}(q, q') \geq (1 + \ell_1)/2$. Hence

$$\bar{K}_{\varepsilon, L}^{n_0}(\bar{V})(q, q') \leq \lambda_0 \bar{V}(q, q') \quad (20)$$

with $\lambda_0 = \lambda^{n_0} + 2b(1 - \lambda)^{-1}(1 + \ell_1)^{-1} < 1$ for all $(q, q') \notin L_{\ell_0}(U_S) \times L_{\ell_0}(U_S)$. Define the subsampled Markov chains $(\tilde{Q}_n^1)_{n \geq 0}, (\tilde{Q}_n^2)_{n \geq 0}$ as $\tilde{Q}_n^1 = Q_{n_0 n}^1, \tilde{Q}_n^2 = Q_{n_0 n}^2$ and the corresponding relaxed meeting time as $\tilde{\tau}_\delta = \inf\{n \geq 0 : |\tilde{Q}_n^1 - \tilde{Q}_n^2| \leq \delta\}$. For integers $n, j \geq 0$, consider the decomposition

$$\text{pr}_{\varepsilon, L}(\tilde{\tau}_\delta > n) = \text{pr}_{\varepsilon, L}(\tilde{\tau}_\delta > n, N_{n-1} \geq j) + \text{pr}_{\varepsilon, L}(\tilde{\tau}_\delta > n, N_{n-1} < j) \quad (21)$$

where N_n denotes the number of times the coupled chain $(\tilde{Q}_k^1, \tilde{Q}_k^2)_{k \geq 0}$ visits $L_{\ell_0}(U_S) \times L_{\ell_0}(U_S)$ by time n (with $N_{-1} = 0$). For the first term, it follows from (18) that

$$\text{pr}_{\varepsilon, L}(\tilde{\tau}_\delta > n, N_{n-1} \geq j) \leq (1 - \omega)^j. \quad (22)$$

To bound the second term, we define

$$B = \max \left\{ 1, \frac{1}{\lambda_0} \sup_{(q, q') \in L_{\ell_0}(U_S) \times L_{\ell_0}(U_S)} \frac{\bar{K}_{\varepsilon, L}^{n_0}(\bar{V})(q, q')}{\bar{V}(q, q')} \right\} \leq \frac{1}{\lambda_0} \left\{ \lambda^{n_0} + \frac{b}{1 - \lambda} \right\} \quad (23)$$

and apply Markov's inequality to obtain

$$\begin{aligned} \text{pr}_{\varepsilon, L}(\tilde{\tau}_\delta > n, N_{n-1} < j) &\leq \text{pr}_{\varepsilon, L} \left\{ \mathbb{I}_{D_\delta^c}(\tilde{Q}_n^1, \tilde{Q}_n^2) B^{-N_{n-1}} \geq B^{-(j-1)} \right\} \\ &\leq B^{j-1} E_{\varepsilon, L} \left\{ \mathbb{I}_{D_\delta^c}(\tilde{Q}_n^1, \tilde{Q}_n^2) B^{-N_{n-1}} \right\} \\ &\leq B^{j-1} E_{\varepsilon, L} \left\{ B^{-N_{n-1}} \bar{V}(\tilde{Q}_n^1, \tilde{Q}_n^2) \right\} \\ &= \lambda_0^n B^{j-1} E_{\varepsilon, L} \{M_n\} \end{aligned} \quad (24)$$

where $M_n = \lambda_0^{-n} B^{-N_{n-1}} \bar{V}(\tilde{Q}_n^1, \tilde{Q}_n^2)$. Let \mathcal{F}_n denote the σ -algebra generated by the random variables $(\tilde{Q}_k^1, \tilde{Q}_k^2)_{0 \leq k \leq n}$. We now establish that $(M_n, \mathcal{F}_n)_{n \geq 0}$ is a super-martingale. Suppose $(\tilde{Q}_n^1, \tilde{Q}_n^2) \notin L_{\ell_0}(U_S) \times L_{\ell_0}(U_S)$, in which case $N_n = N_{n-1}$, and applying (20) gives

$$E_{\varepsilon, L} \{M_{n+1} \mid \mathcal{F}_n\} = \lambda_0^{-n-1} B^{-N_{n-1}} E_{\varepsilon, L} \left\{ \bar{V}(\tilde{Q}_{n+1}^1, \tilde{Q}_{n+1}^2) \mid \tilde{Q}_n^1, \tilde{Q}_n^2 \right\} \leq M_n.$$

For other case $(\tilde{Q}_n^1, \tilde{Q}_n^2) \in L_{\ell_0}(U_S) \times L_{\ell_0}(U_S)$, we have $N_n = N_{n-1} + 1$ hence it follows from (23) that

$$E_{\varepsilon, L} \{M_{n+1} \mid \mathcal{F}_n\} = \lambda_0^{-n} B^{-N_{n-1}-1} \bar{V}(\tilde{Q}_n^1, \tilde{Q}_n^2) \frac{E_{\varepsilon, L} \left\{ \bar{V}(\tilde{Q}_{n+1}^1, \tilde{Q}_{n+1}^2) \mid \tilde{Q}_n^1, \tilde{Q}_n^2 \right\}}{\lambda_0 \bar{V}(\tilde{Q}_n^1, \tilde{Q}_n^2)} \leq M_n.$$

By the super-martingale property and assumption (8), $E_{\varepsilon, L} \{M_n\} \leq E_{\varepsilon, L} \{M_0\} \leq \{(\lambda + 1)\pi_0(V) + b\}/2$. Therefore combining (21), (22), (24) and noting that the relaxed meeting times satisfy $\{\tau_\delta > n_0 n\} \subseteq \{\tilde{\tau}_\delta > n\}$ give

$$\text{pr}_{\varepsilon, L}(\tau_\delta > n_0 n) \leq \text{pr}_{\varepsilon, L}(\tilde{\tau}_\delta > n) \leq (1 - \omega)^j + \frac{1}{2} \{(\lambda + 1)\pi_0(V) + b\} \lambda_0^n B^{j-1}.$$

Since $\lambda_0 < 1$, there exists $m_0 \in \mathbb{N}$ such that $\lambda_0 B^{1/m_0} < 1$. For integer $n \geq m_0$, we can choose $j = \lceil n/m_0 \rceil$ to obtain

$$\text{pr}_{\varepsilon, L}(\tau_\delta > n_0 n) \leq \{(1 - \omega)^{1/m_0}\}^n + \frac{1}{2}\{(\lambda + 1)\pi_0(V) + b\}(\lambda_0 B^{1/m_0})^n$$

which implies (9). \square

Proof of Theorem 2. For any $\delta > 0$, we can apply Proposition 1 with $u_0 = \ell_0$ and any $u_1 \in (\ell_0, \sup_{q \in S} U(q))$; the following adopts the notation in the conclusion of Proposition 1. Suppose that the coupled chain $(X_n, Y_n)_{n \geq 0}$ is initialized at $(X_0, Y_0) = (x, y) \in S_0 \times S_0$ and evolves according to $(X_n, Y_n) \sim \bar{K}_{\varepsilon, L, \sigma}\{(X_{n-1}, Y_{n-1}), \cdot\}$ for all integer $n \geq 1$, $\sigma > 0$ and some $\varepsilon \in (0, \bar{\varepsilon})$, $L \in \mathbb{N}$ satisfying $\varepsilon L < \bar{\varepsilon} \bar{L}$ (note that this differs from the time shift presented in Algorithm 2). Let $\{I_n = 1\}$ denote the event that the coupled Hamiltonian Monte Carlo kernel is sampled from the mixture (11) at time n , i.e. $(I_n)_{n \geq 1}$ is a sequence of independent Bernoulli random variables with probability of success $1 - \gamma \in (0, 1)$. By conditioning on the event $\cap_{n=1}^{n_0} \{I_n = 1\}$, it follows from the proof of Proposition 1 that there exist $n_0 \in \mathbb{N}$ and $\omega \in (0, 1)$ such that

$$\inf_{x, y \in S_0} \text{pr}_{\varepsilon, L, \sigma} \{(X_{n_0}, Y_{n_0}) \in D_\delta \cap S \times S \mid (X_0, Y_0) = (x, y)\} \geq (1 - \gamma)^{n_0} \omega. \quad (25)$$

Now conditioning on the events $\{(X_{n_0}, Y_{n_0}) \in D_\delta \cap S \times S\}$ and $\{I_{n_0+1} = 0\}$, for any $\sigma > 0$ and $\theta_1 \in (0, 1)$, the approximation (10) allows us to select $\delta > 0$ small enough so that the maximal coupling within the coupled random walk Metropolis–Hastings kernel \bar{K}_σ proposes the same value $X_{n_0+1}^* = Y_{n_0+1}^*$ with probability at least $1 - \theta_1$. For any $\theta_2 \in (0, 1)$, we now establish that the probability of accepting the proposed value satisfies

$$\text{pr}_{\varepsilon, L, \sigma} \{X_{n_0+1} = X_{n_0+1}^* \mid I_{n_0+1} = 0, (X_{n_0}, Y_{n_0}) \in D_\delta \cap S \times S, (X_0, Y_0) = (x, y)\} \geq 1 - \theta_2 \quad (26)$$

if $\sigma > 0$ is sufficiently small. We can rewrite the above probability as

$$\text{pr}_{\varepsilon, L, \sigma} \left\{ U_{n_0+1} \leq \min \left[1, \frac{\pi(X_{n_0} + \sigma Z_{n_0+1})}{\pi(X_{n_0})} \right] \mid (X_{n_0}, Y_{n_0}) \in D_\delta \cap S \times S, (X_0, Y_0) = (x, y) \right\}$$

where $U_{n_0+1} \sim \mathcal{U}[0, 1]$ and $Z_{n_0+1} = X_{n_0+1}^*/\sigma \sim \mathcal{N}(0, I_d)$ are independent. By Assumption 4, we have

$$\min \left[1, \frac{\pi(v + \sigma z)}{\pi(v)} \right] \geq \min \left[1, \exp \left\{ -\frac{1}{2} \sigma^2 \beta |z|^2 - \sigma \nabla U(v)^\top z \right\} \right]$$

for all $v, z \in \mathbb{R}^d$. Define $\varphi_1(\sigma, v, z) = \exp\{-\sigma^2 \beta |z|^2 / 2\}$, $\varphi_2(\sigma, v, z) = \exp\{-\sigma \nabla U(v)^\top z\}$ and $B_0(r) = \{z \in \mathbb{R}^d : |z| \leq r\}$ for some $r > 0$. Note that for each $(v, z) \in S \times B_0(r)$ and $i = 1, 2$, $\sigma \mapsto \varphi_i(\sigma, v, z)$ is a monotone function and $\lim_{\sigma \rightarrow 0} \varphi_i(\sigma, v, z) = 1$. Since $S \times B_0(r)$ is compact and ∇U is continuous, it follows from Dini's theorem that $\lim_{\sigma \rightarrow 0} \inf_{v \in S, z \in B_0(r)} \varphi_i(\sigma, v, z) = 1$. By conditioning on the events $\{X_{n_0} \in S\}$ and $\{Z_{n_0+1} \in B_0(r)\}$, we have

$$\left\{ U_{n_0+1} \leq \min \left[1, \frac{\pi(X_{n_0} + \sigma Z_{n_0+1})}{\pi(X_{n_0})} \right] \right\} \supseteq \left\{ U_{n_0+1} \leq \min \left[1, \prod_{i=1}^2 \inf_{v \in S, z \in B_0(r)} \varphi_i(\sigma, v, z) \right] \right\}.$$

The claim in (26) follows by taking $r > 0$ sufficiently large and $\sigma > 0$ sufficiently small. Therefore by symmetry of the coupled chains and Fréchet's inequality, for any $\theta \in (0, 1)$, there exists $\bar{\sigma} > 0$ such that for any $\sigma \in (0, \bar{\sigma})$

$$\text{pr}_{\varepsilon, L, \sigma} \{X_{n_0+1} = Y_{n_0+1} \mid I_{n_0+1} = 0, (X_{n_0}, Y_{n_0}) \in D_\delta \cap S \times S, (X_0, Y_0) = (x, y)\} \geq 1 - \theta. \quad (27)$$

Combining (25) with (27) gives

$$\inf_{x, y \in S_0} \bar{K}_{\varepsilon, L, \sigma}^{n_0+1} \{(x, y), D\} \geq (1 - \gamma)^{n_0} \omega \gamma (1 - \theta) > 0 \quad (28)$$

for $\varepsilon \in (0, \bar{\varepsilon})$, $L \in \mathbb{N}$ satisfying $\varepsilon L < \bar{\varepsilon} \bar{L}$ and $\sigma \in (0, \bar{\sigma})$, where $D = \{(x, y) \in \mathbb{R}^d \times \mathbb{R}^d : x = y\}$. With (28), the claim in (14) follows using the same arguments in the proof of Theorem 1 since the marginal mixture kernel $K_{\varepsilon, L, \sigma}$ satisfies the geometric drift condition

$$\begin{aligned} K_{\varepsilon, L, \sigma}(V)(x) &= (1 - \gamma)K_{\varepsilon, L}(V)(x) + \gamma K_{\sigma}(V)(x) \\ &\leq (1 - \gamma)\{\lambda V(x) + b\} + \gamma\{Q_{\sigma}(V)(x) + V(x)\} \\ &\leq \lambda_0 V(x) + b_0 \end{aligned}$$

for all $x \in \mathbb{R}^d$ and $\sigma \in (0, \min\{\bar{\sigma}, \bar{\sigma}\})$, where $\lambda_0 = (1 - \gamma)\lambda + \gamma(1 + \mu) \in (0, 1)$ and $b_0 = (1 - \gamma)b + \gamma\mu < \infty$. \square

E Verifying assumptions of Theorems 1 and 2

E.1 Model

We consider the posterior distribution of regression coefficients $q \in \mathbb{R}^d$, arising from Bayesian logistic regression with observations $y \in \{0, 1\}^N$ and a Gaussian prior distribution $\mathcal{N}(0, \zeta^{-1}\Sigma)$, where $\zeta > 0$ controls the strength of the prior shrinkage toward zero. We will write the $n = 1, \dots, N$ row of the design matrix $X \in \mathbb{R}^{N \times d}$ as $x_n \in \mathbb{R}^d$.

E.2 Assumptions 4–5

In the above setup, the potential has the form

$$U(q) = \frac{\zeta}{2} q^\top \Sigma^{-1} q + y^\top X q + \sum_{n=1}^N \log\{1 + \exp(-x_n^\top q)\}$$

which is infinitely differentiable. Its derivatives are given by

$$\nabla U(q) = \zeta \Sigma^{-1} q + X^\top y - \sum_{n=1}^N \frac{x_n}{1 + \exp(x_n^\top q)}$$

and

$$\nabla^2 U(q) = \zeta \Sigma^{-1} + \sum_{n=1}^N \frac{\exp(x_n^\top q) x_n x_n^\top}{\{1 + \exp(x_n^\top q)\}^2}.$$

The spectral norm of its Hessian can be bounded by

$$\zeta \nu_{\min}(\Sigma^{-1}) \leq \|\nabla^2 U(q)\|_2 \leq \nu_{\max}(\zeta \Sigma^{-1} + 4^{-1} N \Sigma_X)$$

for all $q \in \mathbb{R}^d$, where $\nu_{\min}(A)$ and $\nu_{\max}(A)$ denote the smallest and largest eigenvalues of a matrix $A \in \mathbb{R}^{d \times d}$ respectively, and $\Sigma_X = N^{-1} \sum_{n=1}^N x_n x_n^\top$ is the Gram matrix. Therefore Assumption 4 is satisfied with $\beta = \nu_{\max}(\zeta \Sigma^{-1} + 4^{-1} N \Sigma_X)$ and Assumption 5 is satisfied on any compact set S with $\alpha = \zeta \nu_{\min}(\Sigma^{-1})$. If we select $\Sigma = \Sigma_X^{-1}$, as considered in Dalalyan [2017a, Example 2], then $\beta = (\zeta + N/4) \nu_{\max}(\Sigma_X)$ and $\alpha = \zeta \nu_{\min}(\Sigma_X)$.

E.3 Geometric drift condition of Hamiltonian Monte Carlo kernel

To establish that the marginal Hamiltonian Monte Carlo kernel satisfies a geometric drift condition (8), we will appeal to [Durmus et al. \[2017, Theorem 9\]](#) which gives sufficient conditions [Durmus et al. \[2017, Assumption H2\(m\)\]](#) on the potential U for geometric ergodicity. We will check the assumptions of [Durmus et al. \[2017, Proposition 6\]](#) to verify [Durmus et al. \[2017, Assumption H2\(m\)\]](#). To do so, we decompose the potential as $U(q) = U_0(q) + G(q)$ with

$$U_0(q) = \frac{\zeta}{2} q^\top \Sigma^{-1} q, \quad G(q) = y^\top Xq + \sum_{n=1}^N \log\{1 + \exp(-x_n^\top q)\}.$$

Firstly, U_0 and G are infinitely differentiable. Secondly, U_0 satisfies $\lim_{|q| \rightarrow \infty} U_0(q) = \infty$, is homogeneous of degree 2 and quasi-convex on \mathbb{R}^d ; see discussion above [Durmus et al. \[2017, Proposition 6\]](#) for precise definitions. Lastly, we need to show

$$\lim_{|q| \rightarrow \infty} \|D^2 G(q)\| = 0 \quad \text{and} \quad \lim_{|q| \rightarrow \infty} \|D^3 G(q)\| \cdot |q| = 0 \quad (29)$$

where D^k denotes the k differential of G and $\|D^k G\|$ is the operator norm of D^k seen as a linear map from the k -fold product space $\mathbb{R}^d \times \cdots \times \mathbb{R}^d$ to \mathbb{R} . Let $|u|_\infty = \max_{i=1, \dots, d} |u_i|$ denote the maximum norm for $u = (u_1, \dots, u_d) \in \mathbb{R}^d$ and equip the product space with the norm $\|u\|_k = \max_{i=1, \dots, k} |u_i|_\infty$ for $u = (u_1, \dots, u_k) \in \mathbb{R}^d \times \cdots \times \mathbb{R}^d$. Note first that

$$\partial_i \partial_j G(q) = \sum_{n=1}^N \frac{\exp(x_n^\top q) x_{ni} x_{nj}}{\{1 + \exp(x_n^\top q)\}^2}, \quad \partial_i \partial_j \partial_k G(q) = \sum_{n=1}^N \frac{\{\exp(x_n^\top q) - \exp(2x_n^\top q)\} x_{ni} x_{nj} x_{nk}}{\{1 + \exp(x_n^\top q)\}^3}, \quad (30)$$

where $\partial_i f$ denotes the partial derivative of $f : \mathbb{R}^d \rightarrow \mathbb{R}$ with respect to the $i \in \{1, \dots, d\}$ coordinate and x_{ij} denotes the $(i, j) \in \{1, \dots, d\}^2$ element of X . For $z = (u, v) \in \mathbb{R}^d \times \mathbb{R}^d$ with $u = (u_1, \dots, u_d)$ and $v = (v_1, \dots, v_d)$ in \mathbb{R}^d , we have

$$\left| \sum_{i=1}^d \sum_{j=1}^d u_i v_j \partial_i \partial_j G(q) \right| \leq |u|_\infty |v|_\infty \sum_{i=1}^d \sum_{j=1}^d |\partial_i \partial_j G(q)| \leq \|z\|_2 \sum_{i=1}^d \sum_{j=1}^d |\partial_i \partial_j G(q)|.$$

Hence $\|D^2 G(q)\| \leq \sum_{i=1}^d \sum_{j=1}^d |\partial_i \partial_j G(q)|$ and the same argument also gives $\|D^3 G(q)\| \leq \sum_{i=1}^d \sum_{j=1}^d \sum_{k=1}^d |\partial_i \partial_j \partial_k G(q)|$. The claim (29) then follows from the tail behaviour of (30).

Having established [Durmus et al. \[2017, Assumption H2\(m\)\]](#), we apply [Durmus et al. \[2017, Proposition 7\]](#) to conclude that the proposal Markov transition kernel with time discretized Hamiltonian dynamics, defined as

$$P_{\varepsilon, L}(q, A) = \int_{\mathbb{R}^d} \mathbb{I}_A\{\hat{\Phi}_{\varepsilon, L}^\circ(q, p)\} \mathcal{N}(p; 0_d, I_d) dp$$

for $q \in \mathbb{R}^d$ and $A \in \mathcal{B}(\mathbb{R}^d)$, satisfies a geometric drift condition, i.e. there exists $\tilde{\varepsilon} > 0$ such that for any $\varepsilon \in (0, \tilde{\varepsilon})$ and $L \in \mathbb{N}$, there exist $a > 0$, $\lambda_P \in (0, 1)$ and $b_P > 0$ such that

$$P_{\varepsilon, L}(V)(q) \leq \lambda_P V(q) + b_P$$

for all $q \in \mathbb{R}^d$ with

$$V(q) = \exp(a|q|). \quad (31)$$

By Durmus et al. [2017, Proposition 5] which also holds under Durmus et al. [2017, Assumption H2(m)], the geometric drift condition for the proposal kernel implies a geometric drift condition for resulting Hamiltonian Monte Carlo kernel, i.e. for all $\varepsilon \in (0, \bar{\varepsilon})$ and $L \in \mathbb{N}$, there exist $a > 0$, $\lambda \in (0, 1)$ and $b > 0$ such that

$$K_{\varepsilon, L}(V)(q) \leq \lambda V(q) + b$$

for all $q \in \mathbb{R}^d$. Note that we retain the same explicit Lyapunov function (31) which will be needed in the following. The finite moment condition $\pi_0(V)$ holds for initial distributions with sufficiently light tails such as Gaussian distributions.

E.4 Excursions from convexity set in Theorem 1

Since Assumption 5 is satisfied on any compact set, we can take $S = B_0(r) = \{q \in \mathbb{R}^d : |q| \leq r\}$ with $r > 0$ arbitrarily large. Under the Lyapunov function (31), the level set conditions in Theorem 1 can be rewritten as

$$B_0(a^{-1} \log \ell_1) \subseteq B_0(r) \cap L_{\ell_0}(U) \tag{32}$$

for some $\ell_0 \in (\inf_{q \in S} U(q), \sup_{q \in S} U(q))$ and $\ell_1 > 1$ satisfying $\lambda + 2b(1 - \lambda)^{-1}(1 + \ell_1)^{-1} < 1$. With $\lambda \in (0, 1)$ and $b > 0$ fixed, the last inequality requires ℓ_1 to be sufficiently large. As $\lim_{|q| \rightarrow \infty} U(q) = \infty$, the latter can be done without violating (32) since we can choose an arbitrarily large ℓ_0 by taking r sufficiently large. This completes the verification of the assumptions required in Theorem 1.

E.5 Remaining assumptions in Theorem 2

For the Gaussian random walk kernel and the Lyapunov function (31), it follows by a change of variables and the triangle inequality that

$$\begin{aligned} Q_\sigma(V)(q) &= \int_{\mathbb{R}^d} \exp(a|q'|) \mathcal{N}(q'; q, \sigma^2 I_d) dq' = \int_{\mathbb{R}^d} \exp(a|q + q'|) \mathcal{N}(q'; 0, \sigma^2 I_d) dq' \\ &\leq \exp(a|q|) \int_{\mathbb{R}^d} \exp(a|q'|) \mathcal{N}(q'; 0, \sigma^2 I_d) dq' \end{aligned}$$

for any $\sigma > 0$ and $q \in \mathbb{R}^d$. Therefore we can take $\mu = \int_{\mathbb{R}^d} \exp(a|q'|) \mathcal{N}(q'; 0, \sigma^2 I_d) dq'$. With μ and $\lambda \in (0, 1)$ fixed, we can define $\lambda_0 = (1 - \gamma)\lambda + \gamma(1 + \mu) < 1$ by taking $\gamma \in (0, 1)$ small enough. Fixing also γ and $b > 0$, the level set conditions in Theorem 2 hold using the same arguments as the previous section. This completes verifying the assumptions required in Theorem 2. Lastly, we note that minor modifications of the above arguments would also show that the assumptions of Theorems 1–2 hold for any multivariate Gaussian target distribution.